JOURNAL OF GEOPHYSICAL RESEARCH, VOL. 111, D18303, doi:10.1029/2005JD006935, 2006

Influence of future climate and emissions on regional air quality in California

Allison L. Steiner,[1] Shaheen Tonse,[2,3] Ronald C. Cohen,[4,5] Allen H. Goldstein,[1] and Robert A. Harley[3]

Received 29 November 2005; revised 24 May 2006; accepted 14 June 2006; published 21 September 2006.

[1] Using a chemical transport model simulating ozone concentrations in central California, we evaluate the effects of variables associated with future changes in climate and ozone precursor emissions, including (1) increasing temperature; (2) increasing atmospheric water vapor; (3) increasing biogenic VOC emissions due to temperature; (4) projected decreases in anthropogenic NOx, VOC, and CO emissions in California for 2050; and (5) the influence of changing ozone, CO, and methane at the western boundary. Climatic changes expected for temperature, atmospheric water vapor, and biogenic VOC emissions each individually cause a 1–5% increase in the daily peak ozone. Projected reductions in anthropogenic emissions of 10–50% in NOx and 50–70% in VOCs and CO have the greatest single effect, reducing ozone by 8–15% in urban areas. Changes to the chemical boundary conditions lead to ozone increases of 6% in the San Francisco Bay area and along the west coast but only 1–2% inland. Simulations combining climate effects predict that ozone will increase 3–10% in various regions of California. This increase is partly offset by projected future emissions reductions, and a combined climate and emissions simulation yields ozone reductions of 3–9% in the Central Valley and almost no net change in the San Francisco Bay area. We find that different portions of the model domain have widely varying sensitivity to climate parameters. In particular, the San Francisco Bay region is more strongly influenced by temperature changes than inland regions, indicating that air quality in this region may worsen under future climate regimes.

Citation: Steiner, A. L., S. Tonse, R. C. Cohen, A. H. Goldstein, and R. A. Harley (2006), Influence of future climate and emissions on regional air quality in California, *J. Geophys. Res.*, *111*, D18303, doi:10.1029/2005JD006935.

1. Introduction

[2] It is widely recognized that maintaining safe atmospheric levels of ozone, carbon monoxide (CO), nitrogen oxides (NO_x), particulate matter and other toxic chemicals depends on both emissions and meteorological conditions. Historically, studies have used projections of emissions and the historical database of meteorological conditions to estimate the effectiveness of emissions reduction policies. However, the policies aimed at reducing the negative impacts of ozone have not accounted for potential climate change [*National Research Council*, 1991] and recent work [*Intergovernmental Panel on Climate Change* (*IPCC*), 2001; *Johnson et al.*, 1999; *Mickley et al.*, 2004; *Hogrefe et al.*, 2004; *Leung and Gustafson*, 2005] indicates that utilizing historical meteorological conditions to determine future air quality is no longer sufficient. By 2050, models project significant changes in global and regional climate, including increases in temperature and changes in the hydrological cycle that will affect the distribution of meteorological conditions. These changes are likely to impact the seasonal cycle by increasing the length and duration of stagnation events that can exacerbate air quality problems [*Mickley et al.*, 2004; *Leung and Gustafson*, 2005]. In this study, we evaluate the relative contributions of several climate change parameters and projected emissions reductions on ozone. As a case study, we investigate how changing physical and chemical parameters influence ozone formation in central California during a 5-day summertime simulation, as well as the synergistic changes that can occur when considering several transformations at once.

[3] In the current climate, two major factors contribute to ozone formation in the troposphere. The first major factor is meteorological conditions such as temperature, atmospheric water vapor, and the presence of stagnant meteorological conditions that favor oxidant accumulation. The second is

[1]Department of Environmental Science, Policy and Management, Division of Ecosystem Sciences, University of California, Berkeley, California, USA.
[2]Environmental Energy Technologies Division, Lawrence Berkeley National Laboratory, Berkeley, California, USA.
[3]Department of Civil and Environmental Engineering, University of California, Berkeley, California, USA.
[4]Department of Chemistry, University of California, Berkeley, California, USA.
[5]Department of Earth and Planetary Science, University of California, Berkeley, California, USA.

0148-0227/06/2005JD006935$09.00

that of emissions, including local effects such as the magnitude and ratio of oxides of nitrogen (NOx = NO + NO_2) and volatile organic compound (VOC) emissions as well as that of global emissions due to intercontinental transport of ozone and its precursors [*Jacob et al.*, 1999].

[4] Future climate has the ability to impact both of these factors via changes in climatic conditions and their impact on surface emissions. Several studies have investigated this interaction using general circulation models (GCMs) to drive global tropospheric chemistry models. Larger global-scale studies such as *Brasseur et al.* [1998] and *Prather et al.* [2003] estimated that future global anthropogenic emissions increases alone would increase near-surface ozone concentrations. However, when changing climate occurs in conjunction with an increase in global anthropogenic emissions, *Brasseur et al.* [1998] and *Johnson et al.* [1999] estimate a slight decrease in surface ozone concentrations on the global scale. Changing climate can also influence surface emissions, particularly biogenic VOC emissions from vegetation. *Sanderson et al.* [2003] found that biogenic VOC emissions increase under future climate scenarios, contributing to an increase in surface ozone concentrations.

[5] However, the impacts on a regional scale are much more complex. Changes in temperature and atmospheric water vapor can increase peak ozone concentrations at the regional level [*Sillman and Samson*, 1995; *Aw and Kleeman*, 2003]. On a seasonal timescale, recent studies have found that changing climate can impact the frequency, length and duration of regional air quality events [*Mickley et al.*, 2004; *Leung and Gustafson*, 2005]. *Hogrefe et al.* [2004] evaluated the relative contributions of climate change versus emissions over the eastern United States, and found that increased intercontinental transport had the greatest impact on the daily 8-hour maximum ozone concentration, but that future climate could have a greater impact than emissions changes on the fourth-highest summertime 8-hour ozone concentration.

[6] The impact of climate change on air quality is likely to vary greatly in different regions. California represents a unique opportunity to study these issues because of the diversity of its landscape and vegetation regimes as well as the distribution of natural and anthropogenic emissions. The impacts of air quality and climate change are also likely to be felt strongly in California, as approximately 1 in 7 United States residents currently live in California and its agricultural regions are some of the most productive in the nation. As of 2004, 35 out of California's 58 counties are designated nonattainment areas for the federal 8-hour ozone standard, with the vast majority of these areas being populated or agricultural regions [*U.S. Environmental Protection Agency* (*USEPA*), 2004]. Therefore air pollution in California is likely affecting more people and agricultural productivity than anywhere else in the United Sates. Furthermore, California population is growing rapidly, and is forecast to increase by approximately 60% between 2000 and 2050 [*California Department of Finance*, 2004].

[7] Several studies have investigated how future climate scenarios would affect temperatures and precipitation in California. The region is considered to be particularly sensitive to climate change, as changes in precipitation and temperature could significantly affect water resources and agriculture. Using resolutions typical for global-scale models, *Coquard et al.* [2004] compared 15 different global climate model runs for a 2 × CO_2 scenario and found an average increase of 2°–3°C over the western United States, with large variability between different models. Regional studies include a dynamically downscaled regional climate run by *Snyder et al.* [2002], which found temperatures increased up to 3.8°C across California under a doubled CO_2 atmosphere. A statistically downscaled study by *Hayhoe et al.* [2004] used two different climate models and two different IPCC SRES scenarios and found temperature increases of 1°–3°C, depending on model, season and IPCC scenario. These studies reinforce the prediction that temperatures will increase in California on the order of a few degrees.

[8] In this study, we examine and compare the effects of regional climate change and future emissions scenarios on ozone formation. We place these two different forces in context by evaluating how changes in chemical composition and climate affect gas phase chemistry in central California. We utilize a three-dimensional model to investigate changes to chemical mechanisms for ozone-producing regimes common in urban and rural areas, allowing our results to indicate potential changes in Central California as well as other regions with similar ozone formation chemistry. While other studies have focused on the seasonal changes affecting the length and duration of ozone events [e.g., *Leung and Gustafson*, 2005; *Mickley et al.*, 2004], we focus here on the impacts of future climate and emissions on the chemical mechanisms occurring during a typical summertime ozone episode in California. We do not include particulate chemistry, though note that it is an important indicator of air quality and future climate is likely to have different impacts on the particulate phase than that of the gas phase [*Aw and Kleeman*, 2003]. Additionally, we do not include the impacts of future land cover changes or biomass burning, which can influence both gas-phase and particulate chemistry [e.g., *Wotawa and Trainer*, 2000]. Our future scenarios consider changes in temperature, absolute humidity, biogenic VOC emissions, anthropogenic emissions, and chemical boundary conditions. We investigate the effects of these parameters on ozone formation by varying them individually and collectively in order to gain insight into the mechanisms of the ozone formation.

2. Description of Model and Methodology

2.1. Model Description

[9] We use the Community Multiscale Air Quality model (CMAQ version 4.3) to perform a 5-day air quality simulation over northern California. CMAQ is a state-of-the-science, three-dimensional air quality model developed by the United States Environmental Protection Agency [*Byun and Ching*, 1999]. In this study, we focus on gas phase chemistry in order to understand the impact of future climate changes on ozone production. Gas phase chemistry is represented with SAPRC99 chemical mechanism [*Carter*, 2000] and the SMVGEAR chemical solver [*Jacobson and Turco*, 1994]. The only change to the chemical mechanism was the addition of methylbutenol (MBO) and its oxidation products, which include aldehydes, acetone, methyl ethyl ketone, formic acid and CO. MBO emissions from Western

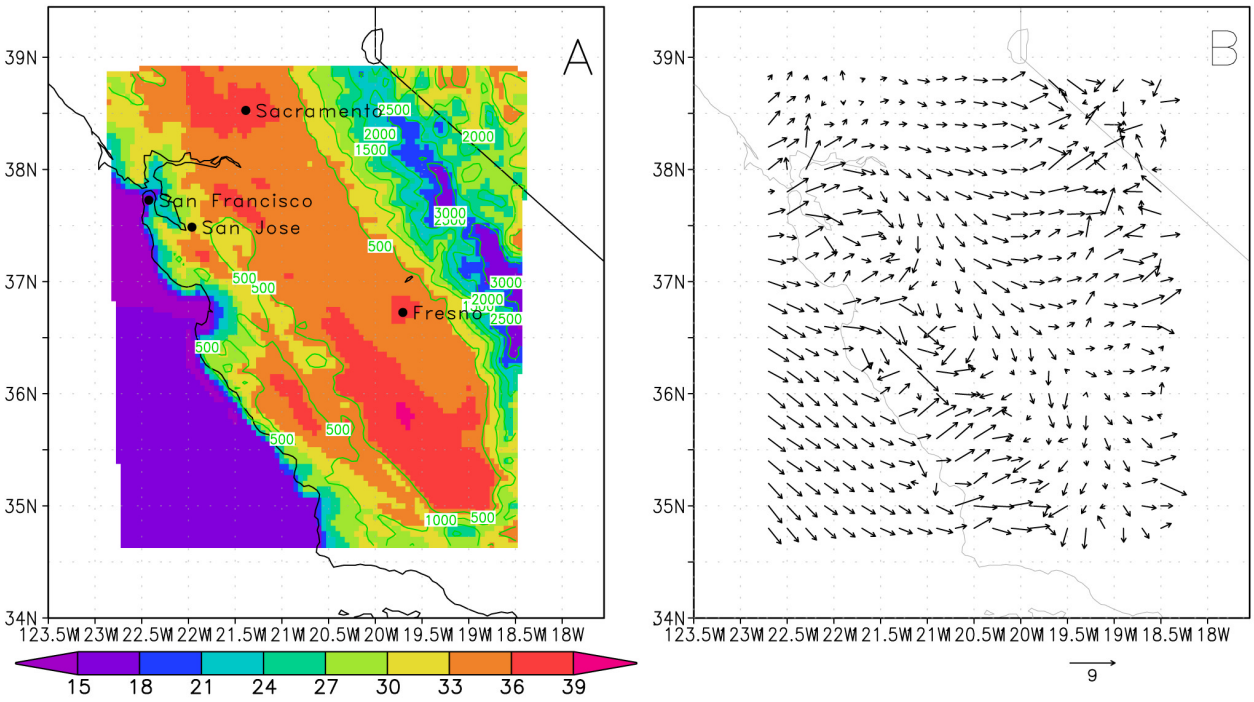

Figure 1. CMAQ model domain, displaying (a) modeled temperature (degrees C) in color with terrain height contours (m) and (b) modeled near-surface (10-m) wind vectors (m/s).

coniferous forests are an important biogenic emission with respect to air quality [*Goldan et al.*, 1993; *Lamanna and Goldstein*, 1999].

[10] Meteorological input to the model is provided by the MM5 meteorological model based on simulations performed for the Central California Ozone Study by J. Wilczak and coworkers (http://www.etl.noaa.gov/programs/modeling/ccos/) from Saturday, 29 July to Wednesday, 2 August 2000. Under typical conditions, central California experiences the inflow of westerlies bringing clean marine air into the region. However, during this summertime ozone episode, a large high-pressure region over Utah and Colorado persisted for several days, creating an offshore pressure gradient that reduced incoming westerly flow and created stagnant conditions favorable to ozone production in the Central Valley [*Fujita et al.*, 2001].

[11] Lateral chemical boundary conditions are supplied to the model to represent the incoming transport of chemical species. We assume temporally constant values of ozone (30 ppb), carbon monoxide (80 ppb), methane (1700 ppb), NO (1 ppb), NO_2 (1 ppb), and a suite of anthropogenic VOCs (approximately 10 ppb). These concentrations are applied to each side of the model domain with constant vertical profile and we note that boundary conditions for NOx, in particular NO, are higher than observed over the Pacific [*Talbot et al.*, 2003; *Hudman et al.*, 2004].

2.2. Model Domain

[12] Figure 1 shows the model domain, which is centered over central California. The model has a horizontal resolution of 4 km, with 96 grid cells in the east-west direction and 117 grid cells in the north-south direction covering approximately 34.5°N to 39°N and 118.5°W to 123°W. This includes the San Joaquin Valley, the San Francisco Bay area, the southern portion of the Sacramento Valley, and the Sierra Nevada mountain range to the east. There are 27 terrain-following vertical sigma layers from the surface to approximately 100 mb, where the first near-surface layer is approximately 20 m. The topography over the region varies widely, including portions of the low-lying Central Valley up to peaks over 3000 m. Average afternoon surface temperatures (Figure 1a) are displayed in conjunction with the complex topography of the region. Afternoon temperatures tend to follow elevation, indicating the strong influence of terrain on our model domain.

[13] Wind vectors in Figure 1b illustrate the average weekday afternoon surface flow based on modeled wind speeds and directions. Northwesterlies over the Pacific tend to run parallel to the coastline, with air moving inland through breaks in the mountain chains. During the daytime, marine air enters the inland portions of California through the Golden Gate and flows southward through the San Joaquin Valley. The wind vectors also show the influence of topography on air flow in the model domain. The coastal mountain chain extending from San Francisco southward to Santa Barbara tends to block incoming air, while the Sierras induce a daytime upslope flow as illustrated by the vectors which reverses to downslope flow during the nighttime (not shown). This indicates that air reaching the inland portions of the state tends to originate from marine air entering through openings in the coastal mountain chain.

2.3. Emissions

2.3.1. Anthropogenic Emissions

[14] Anthropogenic emission estimates were derived from gridded emission inventory data supplied by the California Air Resources Board for a summer 1990 air pollution

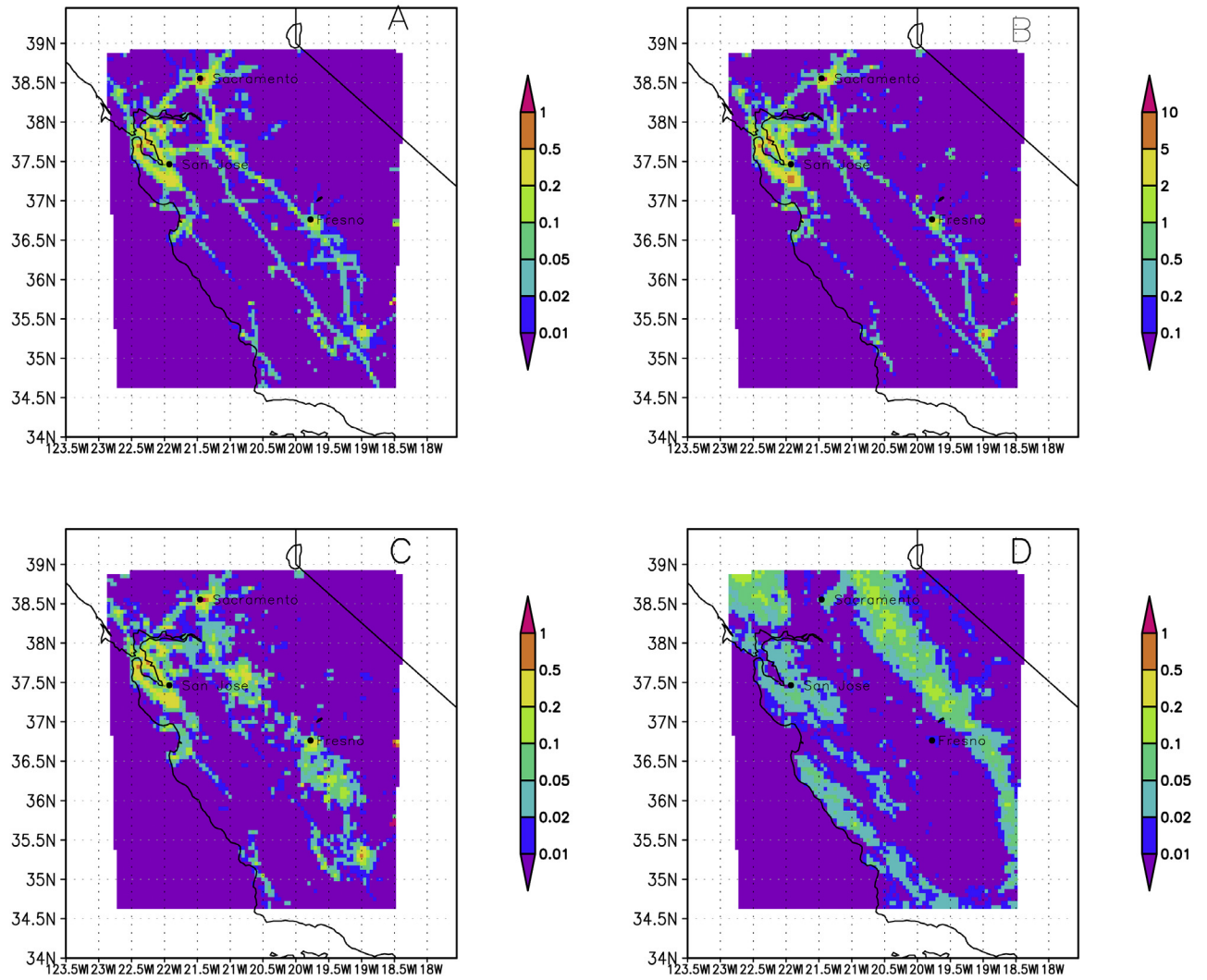

Figure 2. Emissions inputs for CMAQ, 1500 LT average over the three weekdays of the simulation period. (a) NOx emissions (mol/s), (b) CO emissions (mol/s), (c) anthropogenic VOC emissions (mol/s), and (d) biogenic VOC emissions (mol/s).

episode [*Marr et al.*, 2002]. The emission inventory was adjusted to reflect on-road and ambient measurements of pollutant emissions and their ratios, different activity patterns by time of day and day of week, gasoline versus diesel engines, and changes in activity and emissions that occurred between 1990 and 2000 [*Marr et al.*, 2002; *Harley et al.*, 2005]. NOx emissions (shown in Figure 2) include mobile, point and area sources, and the majority of NOx emissions (~80%) in California are from mobile sources. Of the mobile fraction, slightly greater than half are due to diesel emissions and this fraction is expected in increase in the future [*Harley et al.*, 2005]. The weekly NOx emission cycle with reductions on weekends is linked to the major role of diesel exhaust as a source of NOx. Carbon monoxide and anthropogenic VOC emissions are also emitted from point, area and mobile sources, though diesel engines are a minor source. As shown in Figure 2, the highest CO and anthropogenic VOC concentrations are located near urban areas and high-volume transportation corridors. Carbon monoxide emissions tend to be primarily from mobile sources, while all three source types contribute roughly equally to anthropogenic VOC emissions.

2.3.2. Biogenic VOC Emissions

[15] Biogenic VOC emissions are organic compounds emitted naturally from vegetation. The flux of biogenic VOCs to the atmosphere is determined by the amount and type of biomass present, as well as the impact of environmental factors such as light and temperature. In this work, we include biogenic emissions of isoprene, monoterpenes, and MBO. Emissions are estimated hourly over the model domain using the BEIGIS modeling system [*Scott and Benjamin*, 2003], which utilizes detailed land cover data and an extensive emission factor database for California. As shown in Figure 2, the majority of biogenic VOC emissions occur in the forested regions of the model domain, particularly in the foothills of the Sierra Nevadas and in the coastal mountains. Isoprene emissions are the dominant daytime biogenic VOC, with large fluxes arising from oak trees in the Sierra Nevada foothills. Additionally, certain

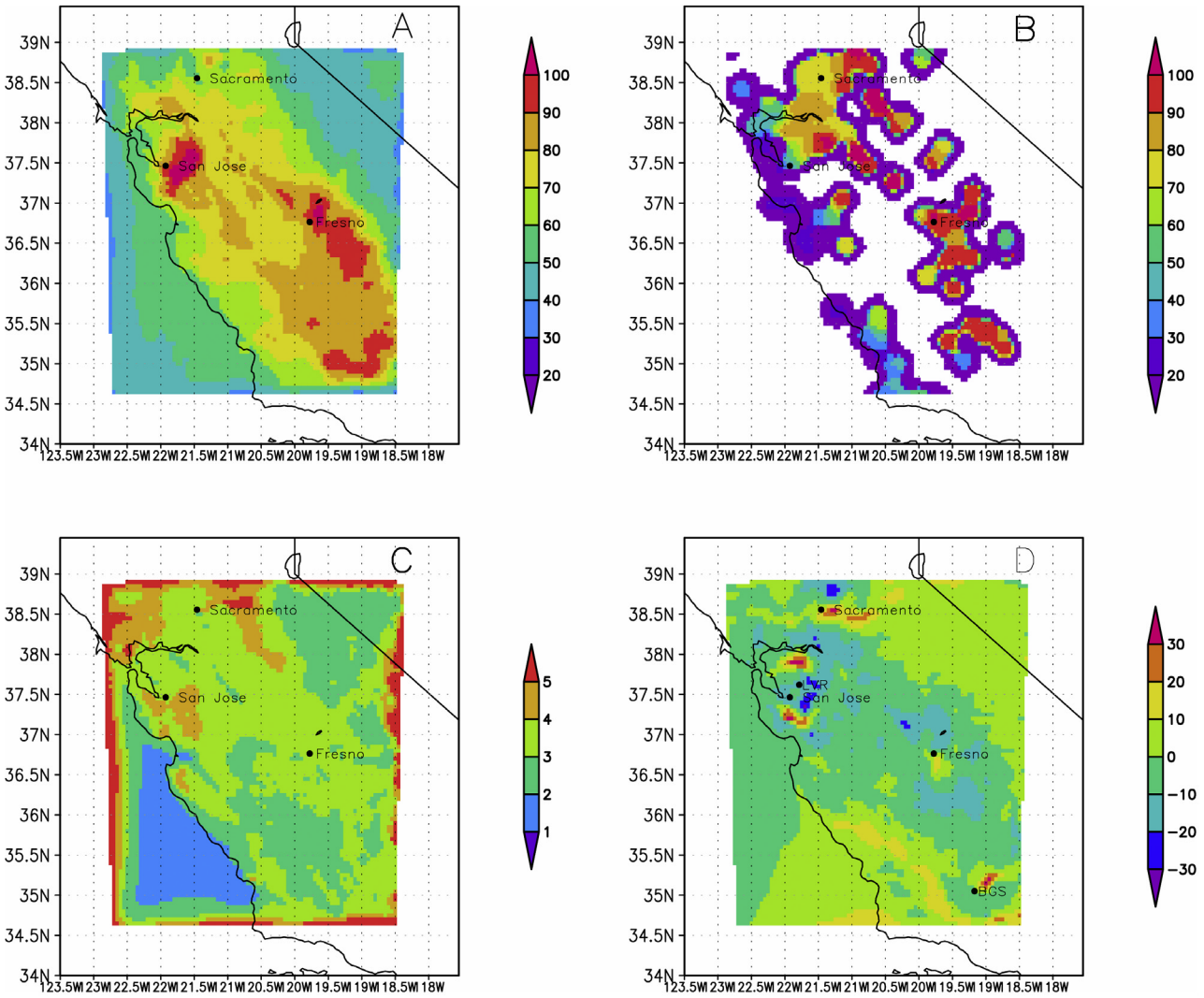

Figure 3. Base case simulation, all figures are weekday averages at 1500 LT. (a) Ozone modeled surface concentrations (ppb); (b) observed, interpolated ozone concentrations (ppb); (c) HOx chain length; and (d) difference between weekend and weekday ozone concentrations ($\Delta(O_{3,weekend} - O_{3,weekday})$) (ppb). Positive values indicate a NOx-saturated regime, while negative values indicate a NOx-limited regime.

crops are emitters of monoterpenes, leading to sources of biogenic monoterpenes in the Central Valley.

[16] Isoprene and MBO emissions occur only in the presence of light, and they increase with solar radiation until a saturation point is reached. Additionally, they both increase exponentially with temperature up to approximately 35°–40°C, after which emissions decrease. In our model, monoterpene emissions increase exponentially temperature and are not dependent on light. These light and temperature effects are represented in the model using parameterizations developed by *Guenther et al.* [1995].

3. Base Case Simulation

3.1. Base Case Ozone and Comparison to Observations

[17] Our base case simulation is a 5-day run over the central California model domain described in section 2, with a 5-day spin-up period. We present results for ozone at 1500 local time (LT), when most locations in the domain exhibit peak ozone concentrations. Because anthropogenic emissions vary greatly between weekdays and weekends, we consider the three weekdays (31 July through 2 August 2000) of the simulation when emissions are greatest. Additionally, concentrations are averaged over the first eleven vertical layers of the atmosphere, representing approximately 250 m above ground level. In the model, the highest ozone concentrations in the domain at 1500 LT occur to the south and east of the San Francisco Bay area (hereinafter referred to as "the Bay area," which specifically refers to the regions with high ozone located in the southern portion of the Bay near San Jose and the eastern portion of the Bay in the vicinity of the Livermore Valley) and in the southern portion of the San Joaquin Valley (Figure 3a), reaching concentrations of ~100 ppb. These high-ozone regions are colocated with regions of high NOx and anthropogenic VOC emissions.

[18] We compare the modeled results for ozone with surface observations from stations throughout California.

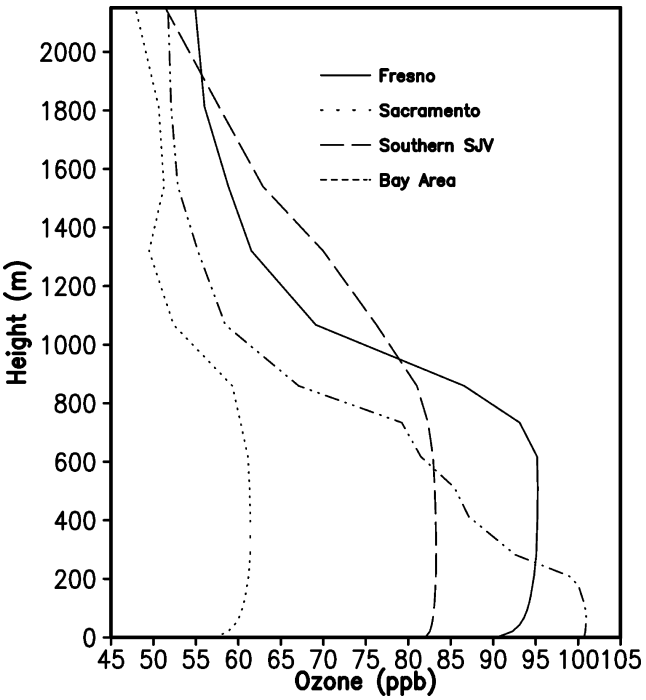

Figure 4. Modeled vertical profiles of ozone concentrations at four locations, 1500 LT weekday average.

Observations at approximately 120 stations within the model domain are interpolated to recreate the observed spatial ozone distribution. The interpolation was performed using a $1/x^2$ distance weighting and a radius of influence of 16 km. While the number of stations in the model domain is limited, this figure provides a picture of how the model reproduces the dominant spatial features of ozone concentrations. In the Bay area, the model over predicts concentrations in the city of San Francisco and the southern portion of the Bay near San Jose by about 30–40 ppb. In the model, this region of high ozone (>100 ppb) covers a large spatial area but with similar maxima to those of the observations. The model also produces ozone that is similar to measurements in the Central Valley.

[19] Observed ozone concentrations in the northern San Joaquin valley and areas upwind of Sacramento in the Sierra foothills are quite high (>90 ppb), while modeled concentrations are lower than the observed (60–80 ppb). This could be due to the lack of a daytime upslope flow in the model carrying ozone and its precursors from the urban regions of Sacramento up to the foothills of the Sierra Nevada, or due to poorly modeled NOx and VOC emissions in this region. Additionally, ozone levels at coastal locations are larger than the observed concentrations, which average 20–30 ppb near Monterey Bay compared to 40–60 ppb in the simulations. Despite these differences in measured versus modeled ozone concentrations, the dominant features of the ozone maxima in the model are colocated with observed ozone maxima and for the most part, the model reproduces measured ozone concentrations.

3.2. Vertical Profiles

[20] Figure 4 shows the vertical profile of concentrations (1500 LT weekday average) for four locations in the model domain. In all cases, ozone concentrations decrease with decreasing height. In Sacramento, concentrations remain nearly constant throughout the boundary layer. In Fresno and the southern San Joaquin Valley, concentrations are well mixed in the first kilometer and then decrease more rapidly with increasing height. In the Bay area, concentrations decrease from the surface and throughout the boundary layer.

3.3. Base Case Chemistry

[21] In the following discussions, the photochemical mechanisms of ozone formation are key to understanding air quality over the region. In the troposphere, the majority of ozone is formed via NO_2 photolysis:

$$NO_2 + h\nu \longrightarrow NO + O(^3P) \quad (1)$$

$$O(^3P) + O_2 \xrightarrow{M} O_3 \quad (2)$$

Ozone formed via this mechanism can be quickly regenerated to NO_2, resulting in no net ozone formation:

$$NO + O_3 \longrightarrow NO_2 + O_2 \quad (3)$$

However, if other atmospheric constituents such as CO and VOCs are present, they can participate in a catalytic cycle that oxidizes NO. In this cycle, VOCs, methane or CO are oxidized by the OH radical to form a suite of peroxy radicals (e.g., HO_2, RO_2) that react with NO:

$$HO_2 + NO \longrightarrow OH + NO_2 \quad (4)$$

$$RO_2 + NO \longrightarrow 2^\circ VOC + HO_2 + NO_2 \quad (5)$$

to generate more hydroxyl and peroxy radicals, NO_2, and secondary VOCs such as aldehydes. This cycle is most often terminated via the self-reaction of peroxy radicals to form peroxides:

$$HO_2 + HO_2 \longrightarrow H_2O_2 \quad (6)$$

$$RO_2 + HO_2 \longrightarrow ROOH \quad (7)$$

by reaction of OH with NO_2 to form nitric acid:

$$OH + NO_2 \longrightarrow HNO_3 \quad (8)$$

or by RO_2 with NO to form alkyl nitrates:

$$RO_2 + NO \longrightarrow RONO_2 \quad (9)$$

Reactions (6)–(9) remove radicals from the system and terminate ozone production. The rate of instantaneous ozone production is affected by the competition for HOx destruction via HOx-NOx reactions when NOx is high (e.g., reactions (8) and (9)) or HOx-HOx reactions when NOx is low (reactions (6) and (7)). When NOx concentrations are low, ozone production tends to increase with increasing NOx and is insensitive to changes in VOC

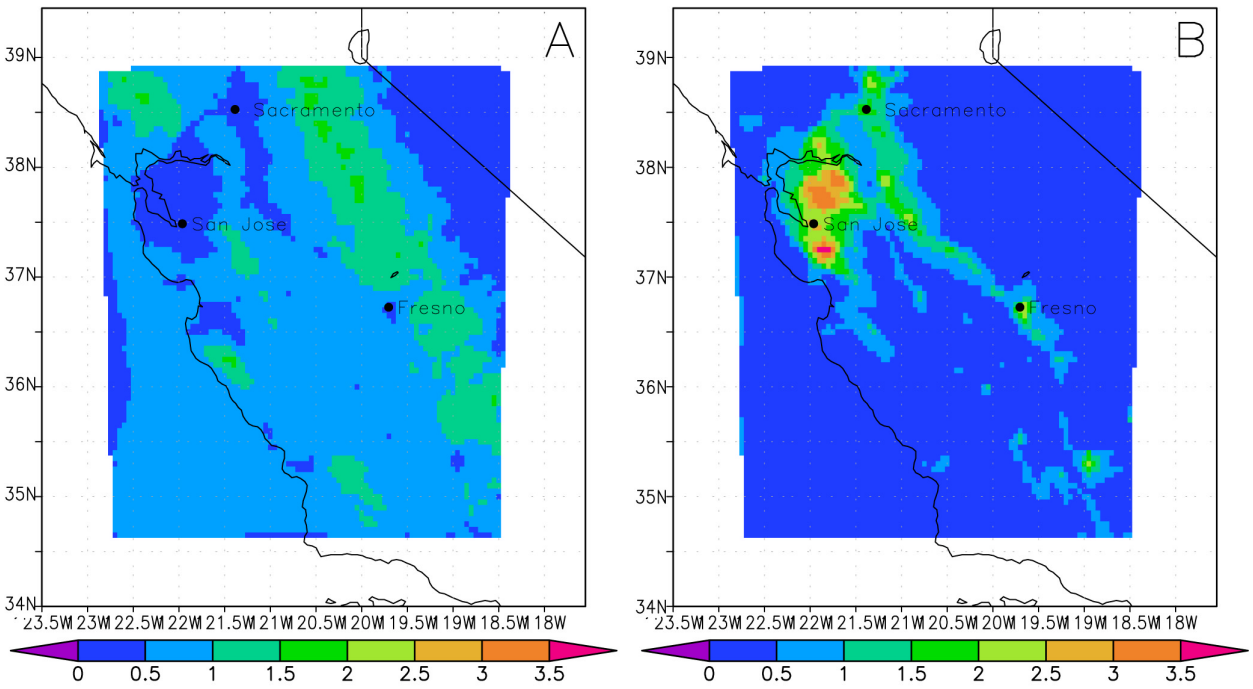

Figure 5. Chemical production rates of chain termination species, 1500 LT weekday average. (a) Peroxide production rates (ppb/hr) and (b) nitric acid production rates (ppb/hr).

concentrations, reflecting a NOx-sensitive environment. When NOx concentrations are high, ozone concentrations are insensitive to NOx and sensitive to changes in VOC concentrations, a regime known as NOx-saturated or VOC-sensitive. The crossover point between these two regions depends on the amount and ratio of VOC and NOx as well as the production of HOx [*Sillman et al.*, 1990; *Sillman*, 1995; *Kleinman*, 1994; *Thornton et al.*, 2002].

[22] Here we define HOx to include OH, HO_2, RO_2, HO_2NO_2, PAN peroxy precursors, and PANs, and P_{HOx} represents the production of new HOx species. In the discussion that follows, ozone concentrations are integrated over the hour and represent an average concentration during this time period, which is more suitable to determine changes to a daily peak concentration of ozone. P_{HOx} can provide insight into the changes in catalytic cycling leading to ozone production and determining the crossover point between NOx-sensitive and NOx-saturated regimes [*Kleinman*, 1986, 1994; *Sillman et al.*, 1990; *Sillman*, 1995; *Thornton et al.*, 2002]. Typically, HOx chain lengths (or the number of times the cycle proceeds before HOx is removed from the system) are about 3–5 in the urban-influenced areas of our model domain (Figure 3c) and are estimated here by the ratio of chain propagation rates (OH + VOC) to chain termination rates (the formation of peroxides and nitric acid).

[23] We use two different markers to determine the chemical regimes in our model domain. The first (Figure 5) compares the chemical formation rate of nitric acid via radical termination steps (indicating the dominance of NOx chemistry) with the formation of peroxides (VOC chemistry). In the Bay Area region as well as in the southern San Joaquin valley, HNO_3 production rates reach 3.5 ppb per hour and concentrations are approximately 5 ppb at the afternoon peak. This indicates the region in which radical chain termination is controlled by HOx-NOx reactions and is NOx-saturated (VOC limited). However, in the mountain regions, peroxide formation is strong indicating that HOx-HOx termination dominates and the regime is NOx-limited.

[24] A second marker of the dominant chemistry regime can be determined by comparing changes in weekday and weekend ozone concentrations, which has been shown to be significant in California [*Cleveland et al.*, 1974; *Altschuler et al.*, 1995; *Marr and Harley*, 2002]. NOx emissions are about 30% greater throughout the domain on weekdays than on weekends, while VOC reactivity varies less than 10% (Murphy et al., The weekend effect within and downwind of Sacramento: Part 1. Observations of ozone, nitrogen oxides, and VOC reactivity, submitted to *Journal of Geophysical Research*, 2006). Comparing weekday and weekend ozone concentrations can give an indication of NOx-limited and NOx-saturated regimes (Figure 3d). If ozone concentrations decrease on weekends ($\Delta(O_{3,weekend}-O_{3,weekday}) < 0$) when NOx is also decreasing, this indicates a NOx-limited regime as decreasing NOx causes a decrease in ozone. On the other hand, if ozone concentrations increase on weekends ($\Delta(O_{3,weekend}-O_{3,weekday}) > 0$) when NOx is decreasing, this indicates a NOx-saturated regime as a decrease in NOx causes an increase in ozone. This marker provides slightly more detail to the general picture of dominant chain termination steps in urban regions. Here, we see strongly NOx-saturated regimes to the south and north of San Jose, in the Sacramento region, and near Fresno and Bakersfield. Figure 6 compares measured and modeled ozone diurnal

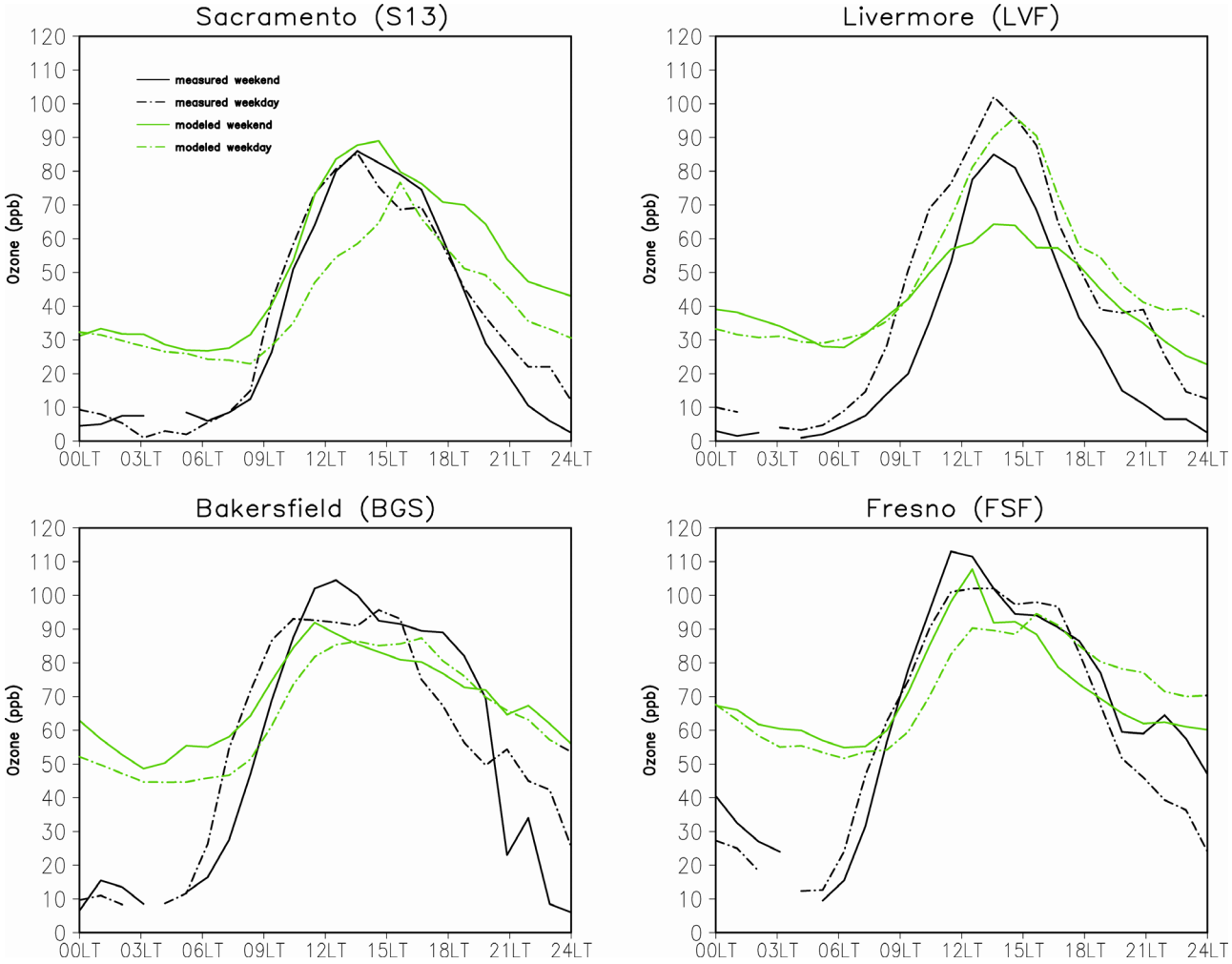

Figure 6. Average diurnal ozone concentrations for weekends (solid line) and weekdays (dashed line) as measured (black lines) and modeled (green lines) for four urban sites. Measurement locations are noted on Figure 3d.

profiles for these regions. At the Sacramento observation site, measured and modeled weekend ozone concentrations are typically higher than the weekday concentrations by approximately 10%, and there is good agreement between the measured and modeled weekday ozone. In the eastern portion of the San Francisco Bay in Livermore, peak weekend ozone concentrations are lower than the weekday values for both the measured and modeled ozone. This reflects the site's location in a portion of the domain where the model predicts that lowering NOx will lower ozone concentrations on the weekend. Both the Fresno and Bakersfield sites show regimes where measured and modeled weekend ozone concentrations tend to exceed weekday concentrations in the morning and late afternoon hours, indicating NOx-saturated regimes.

[25] Together, both markers provide information about the gradient of regimes across the spatial domain, which is important for the sensitivity results and is a key feature of atmospheric chemistry in central California. Understanding the coupling of the NOx regime to climate parameters should also help to understand how climate change would affect locations outside of California.

4. Sensitivity of Air Quality to Climate and Emissions

4.1. Temperature

[26] Under increasing greenhouse gas concentrations, the global mean temperature at the Earth's surface is expected to rise 2°–5°C on the basis of current SRES scenarios [*IPCC*, 2001]. To estimate a future increase in atmospheric temperatures in the model domain, we utilize a regional climate study by *Snyder et al.* [2002]. These simulations use a relatively high resolution model (40 km) to perform an ensemble of regional climate model runs to predict temperatures for two climate scenarios: a preindustrial case, or 1 × CO_2 (280 ppm), and a future 2 × CO_2 case (560 ppm). This represents an overcorrection for temperature, because present-day temperatures are greater than those at preindustrial CO_2 concentrations. However, the temperature perturbations predicted by *Snyder et al.* [2002] are con-

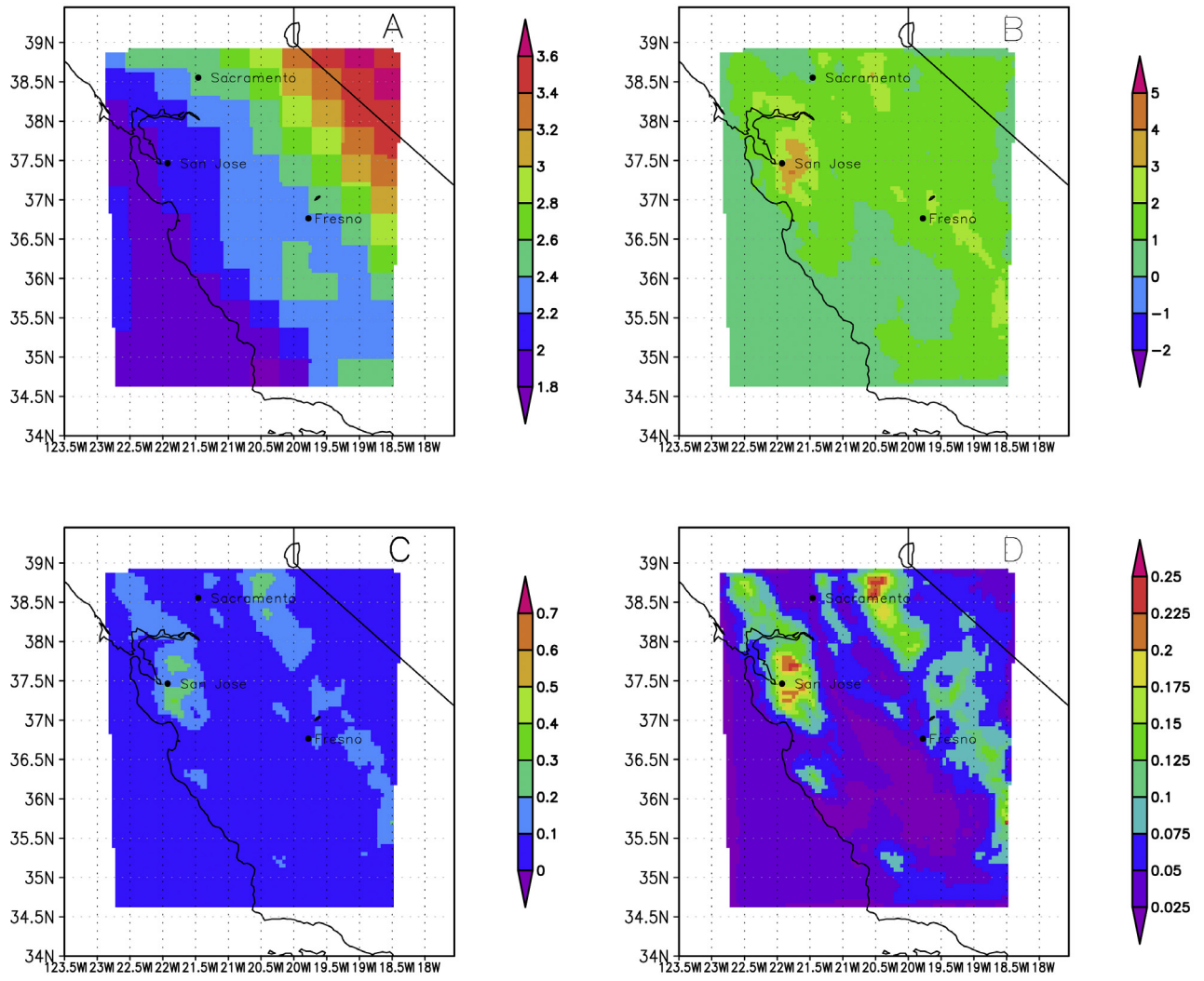

Figure 7. Temperature perturbation, 1500 LT weekday average. (a) Change in temperature (°C), (b) change in ozone (ppb) (temperature simulation – base case simulation), (c) change in HOx production (ppb/hour), and (d) change in formaldehyde concentration (ppb).

sistent with the range of temperature projections by other studies using baseline temperatures from present climatology [e.g., *Hayhoe et al.*, 2004; *Coquard et al.*, 2004]. This modeling study predicts a range of temperature increases over the spatial domain, with increases of ~1°C along the coast to >4°C in the Sierra Nevadas and the eastern portion of the domain (Figure 7a). We use the average August temperature difference between these two simulations to estimate a future temperature increase in our model domain, and have added this temperature change to the MM5 meteorological output utilized by CMAQ. Therefore the temperature change is applied in an uncoupled manner and cannot affect other physical parameters such as wind speed, wind direction, or the boundary layer height. While increased temperatures can have a wide variety of impacts on both physical and chemical processes in the atmosphere, the only impact of temperature in this simulation is via the chemical kinetic reaction rate. Other temperature interactions, such as those that could alter emissions or other physical atmospheric properties are considered separately.

[27] When including the temperature increases described above (Figure 7a), weekday afternoon ozone concentrations increase across the domain (Figure 7b). Increases in ozone range from less than 1 ppb along the coast to up to 2–4 ppb near urban areas. The greatest changes are noted in the regions with high anthropogenic emissions, such as the Bay area, Fresno, and regions downwind of Sacramento. The Bay area has the greatest magnitude of change, with increasing afternoon concentrations of 3–5 ppb (approximately a 3% increase in ozone).

[28] Because the NOx and HOx cycles are tightly coupled, it is difficult to directly attribute changes in HOx and NOx to ozone production. Increasing temperature can affect the VOC + OH reactions depending on whether the reaction occurs because of OH addition or via H abstraction. Alkane + OH reactions occur by H abstraction, a process that increases exponentially with increasing temperature. In contrast, OH addition reactions occur with alkenes and the OH + NO_2 reaction, and these reaction rates tend to decrease with increasing temperature. In the urban areas where we see the greatest increase in ozone concentrations,

anthropogenic emissions are the dominant source of alkanes causing a 3–4% increase in OH reactivity in this region due to an increase in OH + VOC reactions as well as OH + NO_2 reactions. Additionally, secondary formation of formaldehyde can also increase ozone concentrations. Formaldehyde is a secondary product of many VOC reactions with OH (e.g., reaction (4)) and is an effective ozone producer. Figure 7d shows the change in formaldehyde concentrations over the model domain. The greatest increases in formaldehyde concentrations are located in the same regions as ozone changes, confirming that formaldehyde reactions play an important role under increased temperature scenarios. In the Bay area, the contributions to increasing ozone include an increased HOx production, enabling P_{HOx} and OH reactivity to each increase about 2–3%.

[29] At the same time, increasing temperature can increase the decomposition of PANs, freeing up more NOx and HOx radicals for ozone-producing reactions. Past studies have found that increased temperature tends to decrease PANs while increasing NOx and HOx concentrations [*Cardelino and Chameides*, 1990; *Sillman and Samson*, 1995]. In the regions of simulated elevated ozone, the loss of PANs via thermal decomposition increases by about 10–20%. At the same time, we see slight decreases in NOx concentrations and a ~5% increase in the formation of nitric acid and organic nitrates. Thus the additional NOx from PAN decomposition is rapidly converted to more stable NOy reservoirs.

[30] In the regions of increasing ozone, the production of HOx increases approximately 0.1–0.4 ppb per hour (~3.5% increase), with the greatest magnitude of HOx production colocated with that of the ozone increases. Assuming a HOx chain length of 4 and two ozone molecules produced per cycle, this increased source of HOx accounts for up to 3 ppb of the ozone increase. The temperature increase also increases the loss rate of PANs by approximately 1.2–1.5 ppb per hour, which could also contribute to the increased HOx cycling. These two processes are closely coupled, and an increase in VOC reactivity and PAN decomposition are both likely to contribute to increased ozone formation.

4.2. Absolute Humidity

[31] Because warmer air has the capacity to hold more water vapor, one impact of increasing atmospheric temperatures could be an increase in atmospheric water vapor. In order to simulate a change in water vapor, we alter the amount of water vapor (q, or absolute humidity in kg H_2O/kg air) to reflect the temperature changes described in section 4.1. Keeping the relative humidity from the meteorological input constant, we recalculate q for the perturbed temperature [*Wallace and Hobbs*, 2006]. This new value for q is utilized in CMAQ as the amount of water vapor present in the atmosphere, and the spatial distribution of this change is shown in Figure 8a. Changes along the coast are smallest, reflecting the low temperature changes on Figure 7a. Absolute humidity increases with increasing temperature inland and along the foothills of the Sierra Nevada. On the eastern side of the Sierra Nevada Mountains, small increases in absolute humidity occur because of the arid conditions of this region despite large temperature perturbations.

[32] Under elevated atmospheric water vapor, ozone concentrations increase near high anthropogenic emission regions (Figure 8b). The greatest changes occur in the Bay area (1–3 ppb, 1–3%), with enhancements of similar magnitude in and south of Sacramento. These ozone increases are due to amplified HOx production under elevated atmospheric moisture. Water reacts with $O(^1D)$ to form additional OH radicals, injecting more radicals into the HOx cycle and therefore increasing the production of new HOx (Figure 8c). In regions where ozone concentrations are strongly amplified, there is also an increase in loss of VOC (Figure 8d).

[33] In the Bay area, the additional radicals increase NOx-HOx reactions, increasing the NO2 + OH reaction and forming nitric acid (not shown). At the same time, the loss of VOCs increases as well (Figure 8d). In the Bay area, an increase in HOx radicals is more effective at increasing ozone than in Fresno, where NOx concentrations are lower and the region is not as NOx-saturated. In NOx-limited regions such as the eastern portion of the model domain and the Central Valley, ozone decreases slightly. HOx production increases throughout the Central Valley and into the foothills of the Sierras, yet low NOx allows these radicals to increase the production of peroxides (not shown). The increase in peroxides removes radicals from the system, causing a slight reduction of ozone in NOx-limited portions of the domain.

4.3. Biogenic VOC Emissions

[34] Isoprene and MBO emissions increase with increasing temperature until ~37°C and then decrease with increasing temperature, while monoterpene emissions are exponentially dependent on temperature. Some biogenic VOCs such as isoprene and MBO are also dependent on the amount of incoming solar radiation. However, summertime is the dry season in California, with very little convective activity, large-scale frontal systems, and cloud cover. In the present climate, daily amounts of solar radiation reaching the surface show little variability, and we do not expect this forcing to change much during future summer seasons (excluding the impacts of future aerosol events). Thus, for biogenic VOCs a temperature change should capture most of the effects of a future climate in California.

[35] In this sensitivity test, we use the temperature increase described in section 4.1 (Figure 7a) to drive the biogenic emissions model (as described in section 2.3.2). The result is an increase in biogenic emissions throughout the model domain (Figure 9a). Biogenic emissions typically increase by 20–30%, with 30–45% increases in the high mountain elevations, consistent with the increasing temperature change from the coast to the mountains. On an absolute change basis, the greatest magnitude of emissions increases in biogenic emissions are generally where the emissions are the strongest, such as the oak tree band of isoprene emissions stretching from northwest to southeast in the Sierra Nevada foothills.

[36] The greatest impact on ozone from increasing biogenic VOC emissions occurs in the Bay area, where biogenic VOC emissions are modest (ranging from 2 to 6 mol/s per grid square at midday). Ozone in this region increases about 3–5 ppb (approximately 3–5%) and about

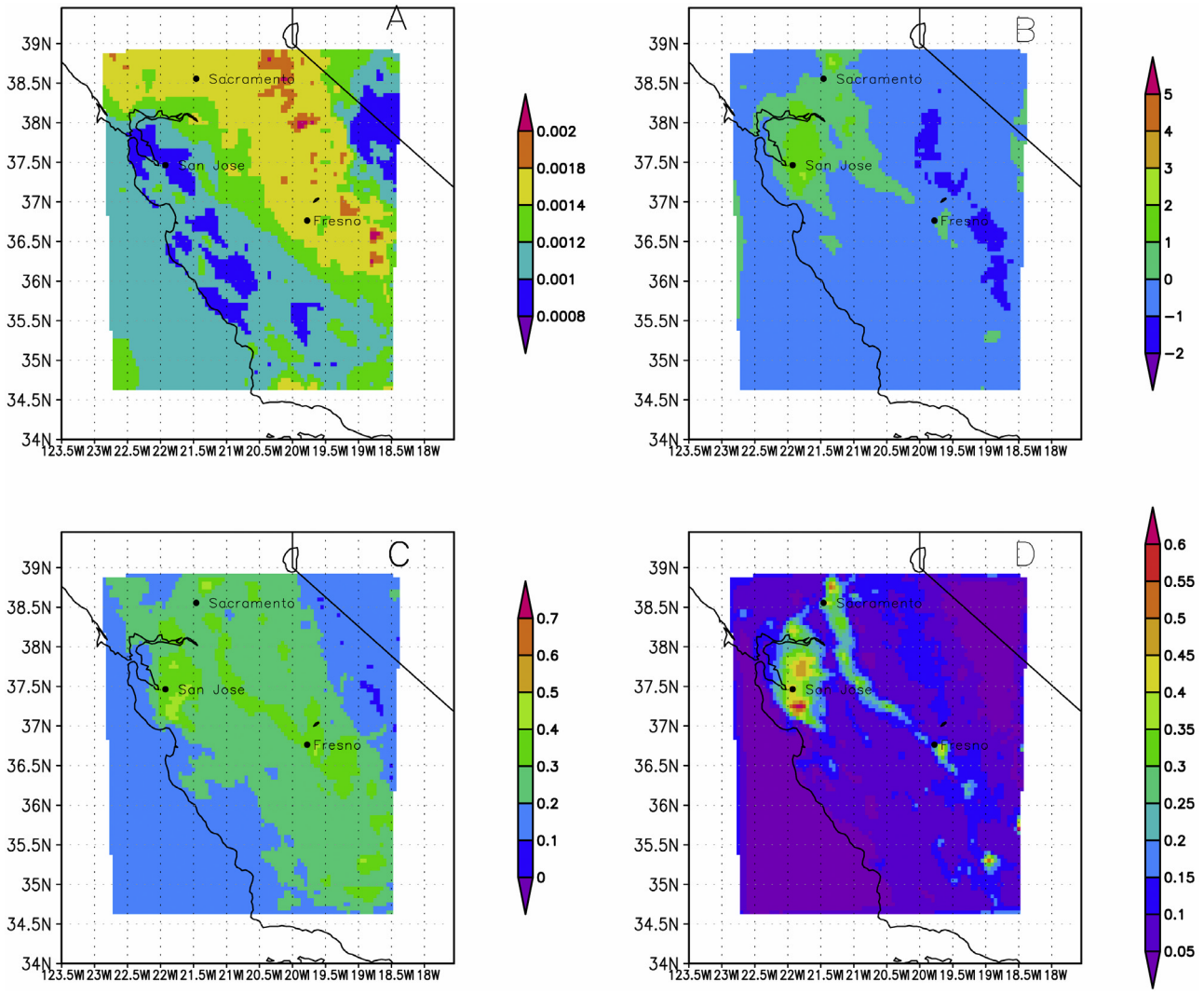

Figure 8. Specific humidity perturbation, 1500 LT weekday average. (a) Changes in q (g/kg), (b) change in ozone concentrations (ppb), (c) change in HOx production (ppb/hr), and (d) change in VOC loss (ppb/hr).

0–2 ppb throughout the Central Valley, while ozone in the mountains decreases slightly (<1 ppb). Ozone increases are much more prominent in the Bay area than they are in other urban regions with similar baseline ozone concentrations and emissions. As with its response to the temperature and humidity perturbations, one of the reasons that the Bay area experiences larger ozone changes is an increase in HOx cycling in this NOx-saturated regime. This difference in regime is highlighted by the comparison of HNO_3/peroxide chemistry shown in Figure 5. In the Bay area, chain termination is strongly dominated by nitric acid formation, with very little formation of peroxides. In contrast, other high-ozone regions such the southern San Joaquin Valley exhibit both nitric acid formation and peroxide formation. Adding biogenic VOCs into the atmosphere in VOC-limited (NOx-saturated) regimes such as the Bay area enhances OH, RO_2 and ozone production. This increase in OH concentrations causes a decrease in NOx lifetimes and increases the production of O_3 per NOx emitted. Overall, these results indicate that a climate change induced increase in biogenic VOC emissions will have a strong influence in NOx-saturated (VOC-limited) urban locations, resulting in higher ozone. This is a result consistent with earlier analyses of correlating temperature and ozone in the Eastern United States [*Sillman and Samson*, 1995]. In rural areas, increased biogenic VOCs will result in a slight decrease in ozone because of reduced NOx concentrations from increased reactivity in the urban source areas. This decrease of incoming NOx leads to less NOx availability for ozone production in rural areas, resulting in more rapid peroxide chain termination. This is evident in the increase in the chemical production rate of peroxides in the Sierras, which is colocated with a slight decrease in ozone (Figure 9d).

4.4. Anthropogenic Emissions in 2050

[37] In this simulation, anthropogenic NOx (here as NO + NO_2), CO and VOC emissions are projected to the year 2050. These predictions are derived for mobile, area and point sources for each air basin delineated within our model domain. Future projections are based on a combination of two factors: (1) increases in population growth that lead to

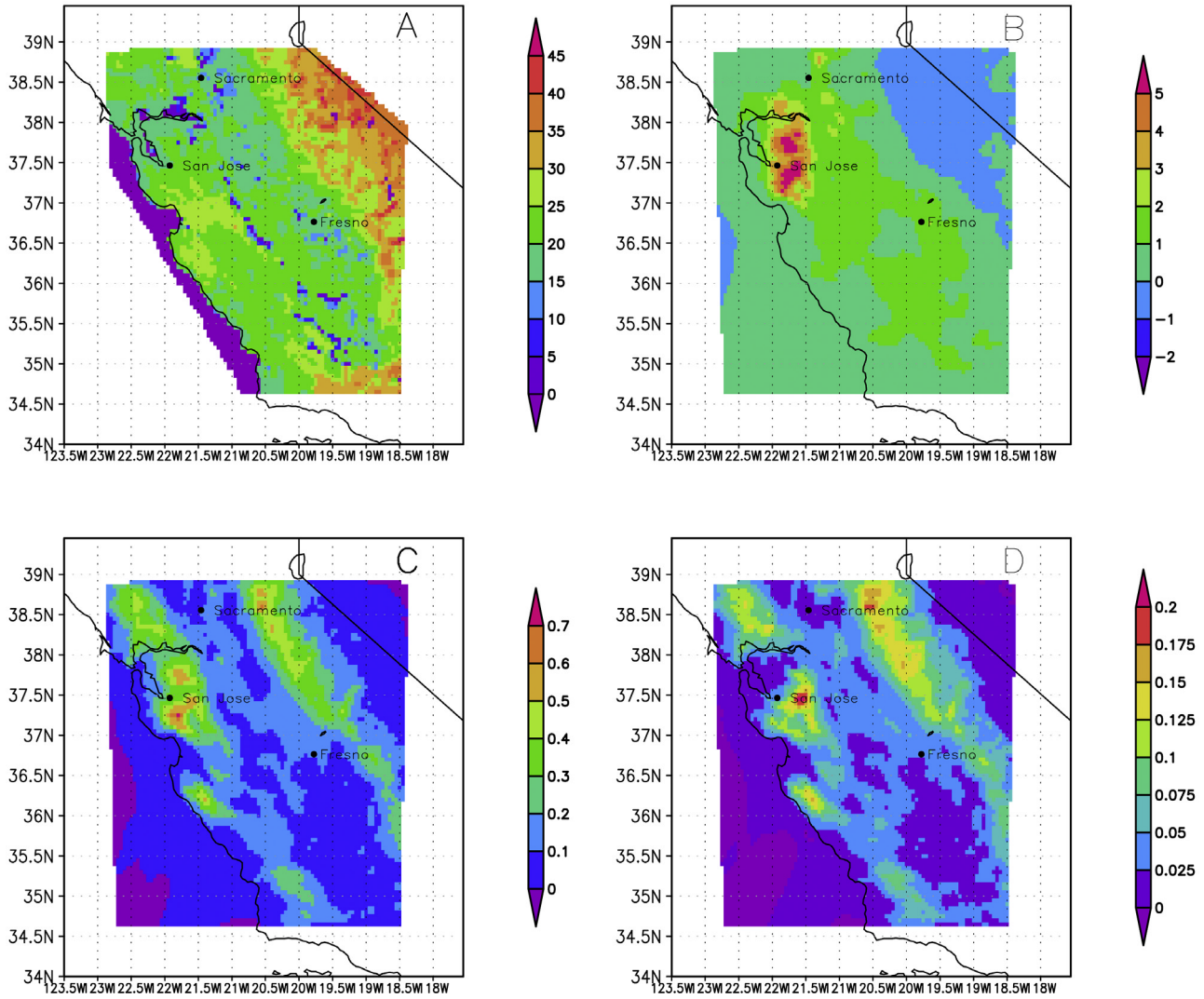

Figure 9. Biogenic VOC perturbation, 1500 LT weekday average. (a) Percent change in biogenic VOC emissions, (b) change in ozone concentration (ppb), (c) change in HOx production (ppb/hr), and (d) change in peroxide concentrations (ppb).

increases in pollution-causing activities and (2) decreases in emissions factors due to advances in technology (Table 1). Here we assume 80% reductions in emission factors below present-day (2000) values. This implies an increase in overall control effectiveness from ~90% to 98% for CO and VOC, and from ~40% to 90% for NOx between the years 2000 and 2050.

[38] Population growth by air basin has been projected by county out to 2050 [*California Department of Finance*, 2004]. In general, increases in fuel usage that affect CO, VOC, and NOx emissions tend to follow that of population growth [*USEPA*, 2005], therefore we use population as a proxy in estimating future fuel consumption. In Table 1, VOC and CO emission scaling factors reflect both population growth and reduced emission factors. For NOx emission factors, diesel fuel usage has been growing approximately three times faster than gasoline [*Harley et al.*, 2005]. We therefore estimate the effect of growth on NOx emissions will be twice that for the other pollutants, assuming that two thirds of the NOx emissions are attributed to diesel fuel usage (growing at a factor of 3) and one third of fuel usage is from gasoline emissions (growing at a factor of 1). Diesel engines are a minor source of CO and VOC. VOC and CO emissions decrease by 50–70% in the Central Valley, where population is expected to double by 2050 (Figure 10a). In contrast, population growth is expected to increase by only 50% in the Bay area, leading to VOC and CO reductions of 70% from present-day emissions. NOx emission reductions are not as large (Figure 10b). In the Central Valley, NOx decreases about 10–20%, while emissions along the coast decrease from 30 to 50%.

[39] Reductions in anthropogenic emissions have a larger impact on ozone compared to the other simulations. The greatest reductions in ozone concentrations occur in urban areas, with decreases of 15–20 ppb in the Bay area and surrounding Fresno (Figure 10c). Throughout the southern San Joaquin Valley, decreases range from 5 to 10 ppb. We compare weekend and weekday ozone concentrations (Figure 10d) and find that the overall spatial distributions of NOx-saturated versus NOx-limited regimes does not

Table 1. Emission Scaling Factors for 2050 Anthropogenic Emissions Relative to Present-Day Conditions (Summer 2000)[a]

Air Basin	Population Growth Factor	VOC and CO Scaling Factor	NOx Scaling Factor
San Francisco Bay	1.48	0.30	0.59
Sacramento Valley	2.19	0.44	0.88
San Joaquin Valley	2.39	0.48	0.96
Mountain Counties	2.03	0.41	0.81
North Coast/Lake County	1.56	0.31	0.62
North Central Coast	1.47	0.29	0.59
Northeast Plate	1.03	0.21	0.41
South Central Coast	1.35	0.27	0.54
Great Basin Valley	1.17	0.23	0.47
Mojave Desert	1.95	0.39	0.78

[a]For gasoline emissions, fuel use growth is expected to follow the population growth factor, therefore VOC and CO emission factors are equal to the population growth factor times 0.2. More rapid growth in diesel fuel usage is assumed, leading to smaller reductions in NOx emissions (see text).

change significantly as compared to that of the base case simulation (Figure 3d). This is expected in the Central Valley, as NOx emissions are only reduced 10–20%, however significant reductions of NOx in the San Francisco Bay area of 40–50% do not convert the region from a dominantly NOx-saturated regime to one that is NOx-limited. This indicates that while the emissions reductions cause significant changes in ozone, there is not a shift in the dominant chemistry in our urban locations.

[40] This case represents the potentially large influence of emissions reductions in central California. Emission reductions in the Central Valley (NOx reductions of 10–20% and VOC/CO reductions of 50–60%) decreased ozone throughout the region by 10–15%. Similarly, for the Bay area, where reductions in emissions were slightly greater than in the Central Valley, ozone was reduced by 15%. The sensitivity of ozone to VOC changes is evident by examining the change in VOC reactivity (Figure 10e). In the Bay area, VOC reactivity slows by about 4–5 ppb/hour in locations where ozone decreases about 16–20 ppb, indicating that VOC reactivity changes account for about one half of the ozone reductions.

4.5. Inflow Boundary Conditions

[41] In a limited area chemical transport model, concentrations of ozone and ozone precursors are specified at each of the model domain boundaries to represent inflow of pollutants. Rising anthropogenic emissions and the resulting formation of ozone over Asia and the North Pacific have already lead to an increase in ozone and its precursors transported into California, and Asian emissions are projected to increase in the coming decades [*Jacob et al.*, 1999; *Holloway et al.*, 2003; *Goldstein et al.*, 2004; *Parrish et al.*, 2004]. In the base case scenario, boundary conditions on all sides of the model domain are set at 30 ppb for ozone, 80 ppb for CO, 1.7 ppm for methane, 1 ppb for NO_2, and 1 ppb for NO. The dominant airflow pattern into the model domain is incoming westerlies from the Pacific Ocean (Figure 1b) therefore we focus on changes in concentrations along the western boundary of the model domain. In this simulation, we elevate the concentrations of CO, ozone and methane at the western boundary in order to estimate the impact of increasing pollutants from the western boundaries.

[42] To estimate future concentrations for this simulation, we scale current boundary condition concentrations to reflect future emissions and global concentrations. We base this projection on the A1B emission scenario of the IPCC report [*IPCC*, 2001] for CO and methane. In this future emissions scenario, CO emissions are expected to increase from 877 to 1214 Tg CO/year between 2000 and 2050, therefore we increase CO concentrations by roughly 30%, or from 80 to 104 ppb. For methane, concentrations are projected to increase to 2400 ppb in 2050, reflecting an increase of about 30%. Exceptions to the A1B projections include NOx and ozone. NO and NO_2 are held at values of 1 ppb as this already represents a large value for NOx entering the domain. We increased ozone concentrations from 30 ppb in the base case run to 40 ppb in the 2050 estimation, reflecting a 30% increase. This is larger than the 15% increase in background ozone concentrations predicted by the A1B scenario, and we roughly doubled the projected increase in order to investigate effects of both an increase in global background ozone concentrations and the specific potential for higher ozone reaching the Pacific Coast from increasing precursor emissions in Asia.

[43] The influence of the chemical boundary conditions depends on physical and chemical factors. Physical parameters such as proximity to the model boundary and dominant wind patterns can affect the ozone imported from the west. The dominant westerlies are typically blocked from moving inland by the mountain chains along the California coast, although air can reach inland through one of several gateways that occur at breaks in the coastal mountain ranges. Modeled chemistry also influences the spatial distribution of ozone. In this simulation, OH concentrations are high (afternoon average OH concentrations range from 2×10^6 molecules/cm^3 in rural areas to $1–2 \times 10^7$ near high-emission regions and the model boundaries) and the chemistry in the region progresses at a relatively fast rate. Figure 11c shows the base case rate of production of Ox species (defined as $Ox = O_3 + NO_2 + O(^3P) + O(^1D) + HO_2NO_2 + 2*NO_3 + 3*N_2O_5 + PANs$), indicating the high rates of production along the western boundary and near high-emission regions. Ozone lifetimes are estimated to be in the range of 3–8 hours. Therefore local chemistry is occurring quickly and there is limited memory of the boundary conditions.

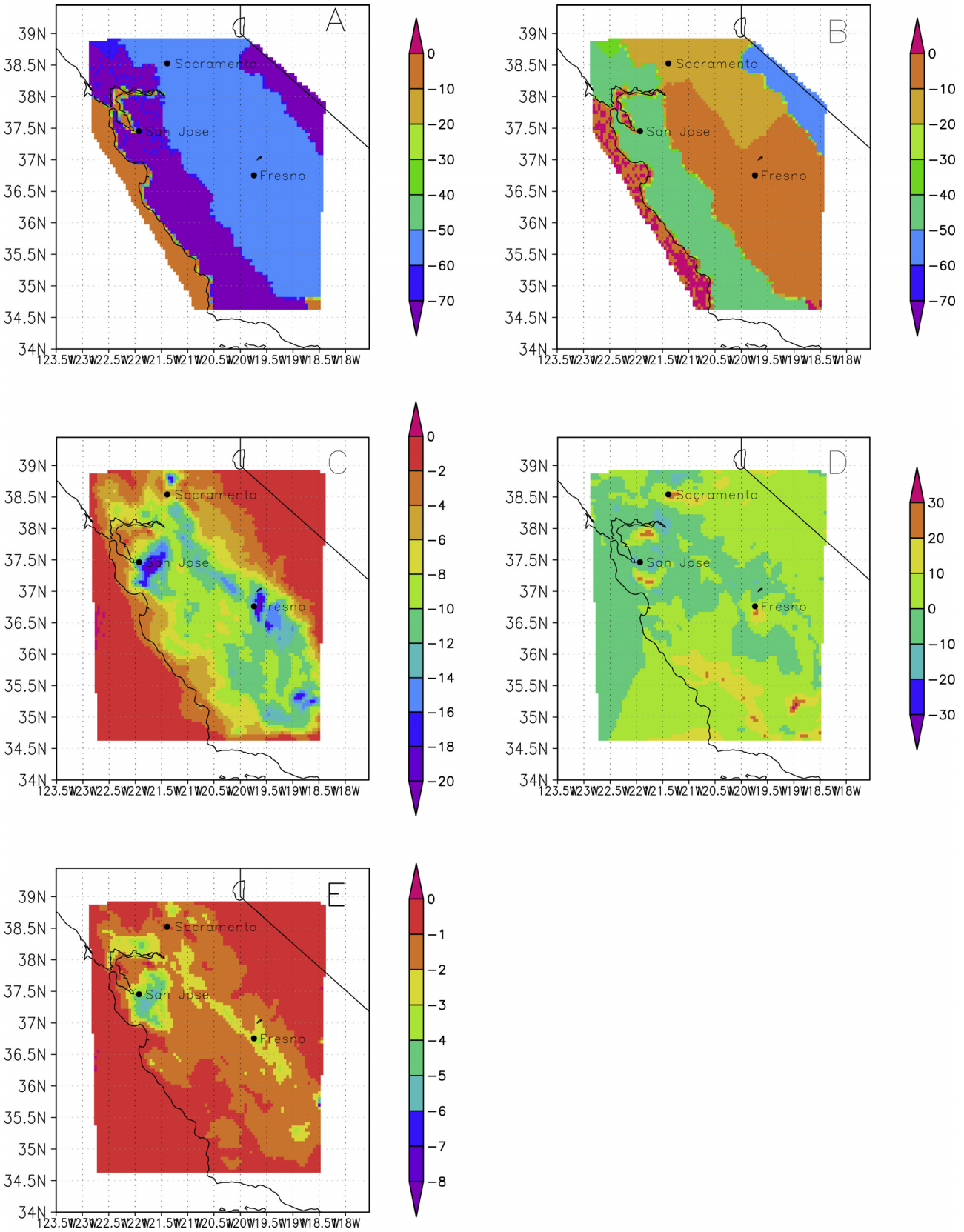

Figure 10. Projected anthropogenic 2050 emissions, 1500 LT weekday. (a) Percent change in anthropogenic VOC and CO emissions, (b) percent change in anthropogenic NOx emissions, (c) change in ozone concentrations (ppb), (d) change in VOC reactivity (ppb/hr) and (e) difference between weekend and weekday ozone concentrations ($\Delta(O_{3,weekend} - O_{3,weekday})$).

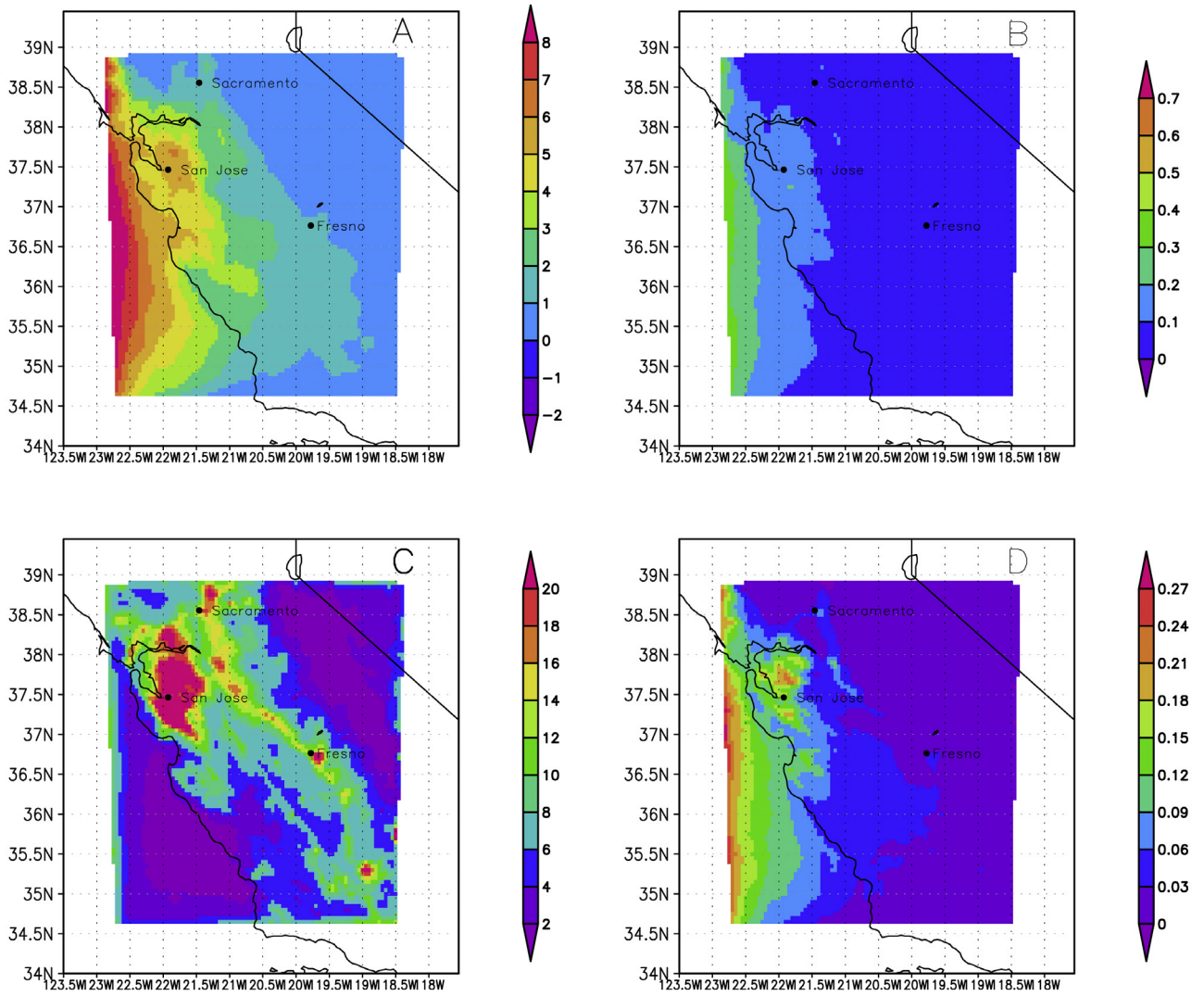

Figure 11. Inflow boundary condition, 1500 LT weekday average. (a) Changes in ozone concentrations (ppb), (b) changes in HOx production (ppb/hr), (c) the base case gross Ox production rate (ppb/hr), and (d) the change in the Ox loss rate (ppb/hr).

[44] Figure 11 illustrates the average weekday change in ozone concentrations and HOx production between this simulation and the base case. As air moves from the western border to the coastline, high OH concentrations and fast chemistry lead to the increased chemical loss of Ox (Figure 11d). Ozone concentrations in the San Francisco Bay area increase up to 7 ppb, partly because of increased transport from the boundary and partly because of an increase in local chemical production from the increase in HOx radicals and accelerated chemistry. The chemical production is calculated to contribute approximately 2 ppb to the total ozone change in this region. Air also moves inland via the break in the coastal mountain chain in the Monterey Bay region, causing ozone concentrations to increase up to 6 ppb in this area with a negligible increase in local chemical production. The extent of the boundary condition influence continues to decrease as air moves eastward in the model domain. Air moving through the San Francisco Bay area penetrates into the Central Valley, where it is then transported north into the Sacramento Valley and south into the San Joaquin Valley, depending on the airflow. Ozone in the Central Valley increases by about 1–2 ppb when averaged over the three simulated weekdays. In the Sierra Nevada, ozone increases are slight (<1 ppb), indicating that the impact on the rest of the model domain is minimal. The influence of the western boundary is not significant in the urban regions of Sacramento and Fresno, as a chemical loss of ozone removes the impact of the western boundary as air is transported inland (i.e., chemical loss rates > transport rates).

[45] An important caveat to this simulation is the dominant meteorological conditions during the simulation. As discussed in section 2.1, a large high-pressure region controlled circulation patterns during the simulation period and reduced the amount of westerly flow and clean marine air entering the Central Valley, a situation conducive to producing high ozone. During situations with stronger westerly flow it is possible that the boundary conditions would propagate further into the domain, however we expect a stronger influence of the boundary to be coupled with lower ozone overall. For example, *Jacob et al.* [1993]

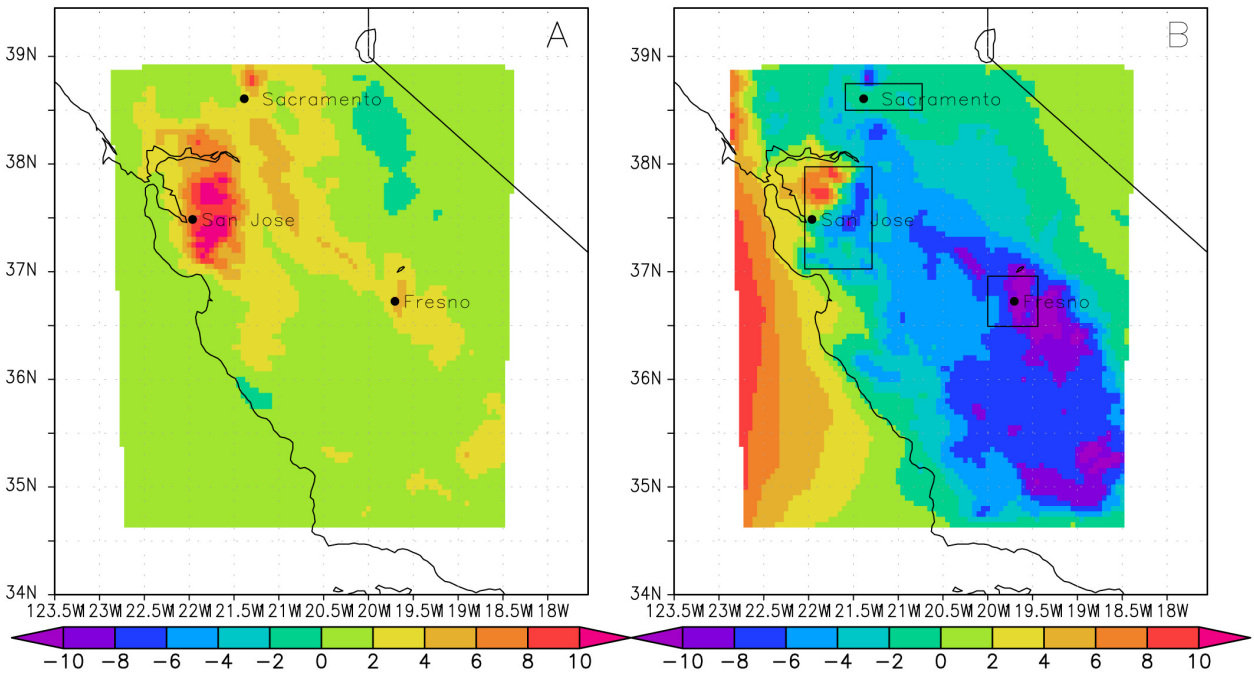

Figure 12. Ozone concentration change from combined simulations, 1500 LT weekday average for (a) combined climate parameters (temperature, humidity, and biogenic VOC emissions) and (b) climate and emission parameters (temperature, humidity, biogenic VOC emissions, boundary conditions, and anthropogenic emissions). Boxes represent the regional averages for Sacramento, Fresno, and the eastern portion of the San Francisco Bay.

calculate that US-produced ozone is important to average ozone concentrations in Europe, but that it made a much smaller contribution during stagnation events that lead to local ozone production.

4.6. Combined Simulations

[46] For the combined simulations, we display the average ozone change for two scenarios (Figure 12). In the first simulation (or "combined climate" scenario), we combine three individual climate-only changes: the temperature change (section 4.1), the absolute humidity change (section 4.2), and the biogenic VOC emissions change (section 4.2). The second simulation (or "climate and emissions" scenario) accounts for both climate change and anthropogenic influences, including the five previous effects in one simulation: temperature, absolute humidity, biogenic VOC emissions change, anthropogenic emissions reductions in 2050 (section 4.4), and changes to the western boundary condition (section 4.5). Because this is not a fully coupled chemistry-climate run, other synergistic effects resulting from future temperature (changes in wind parameters, boundary layer height, and cloud formation) are not included in these simulations.

[47] In the combined climate simulation, the impact of temperature is allowed to influence the chemical kinetic rates, specific humidity and the emission of biogenic VOCs. This causes a substantial increase of up to 10 ppb ozone in the Bay Area and near other locations of high emissions (Figure 12a). In accordance with the biogenic VOC simulation, there are slight depressions in ozone in rural regions where biogenic VOC reactivity dominates. In the climate and emissions simulation, the reduction of anthropogenic emissions and the influence of the western boundary condition dominate the changes in ozone concentrations (Figure 12b). Ozone is reduced throughout the inland areas. For example, average ozone concentrations in the southern San Joaquin Valley are reduced by up to 10 ppb, because of the strong influence of reductions in anthropogenic emissions. However, the influence of boundary conditions is the dominant feature in coastal regions, particularly the San Francisco Bay area, where ozone increases by about 6–8 ppb.

5. Discussion

[48] In order to compare the relative impacts of the climate and emission changes described in section 4, we examine three regions in central California: Sacramento, Fresno, and the area to the south and east of San Francisco Bay (outlined in Figure 12b). We focus on these regions because they (1) have high ozone concentrations in our base case episode, (2) have a history of ozone exceedance events, and (3) exhibit different regimes along the NOx-limited/NOx-saturated continuum. In the San Joaquin Valley air basin where Fresno is located, there are typically over 100 exceedances of the 1-hour ozone national and state standard each year, with a similar number of exceedances of the 8-hour national average. The frequency of high-ozone days in the Central Valley is already very high, so this region is not likely to be strongly impacted by changes in

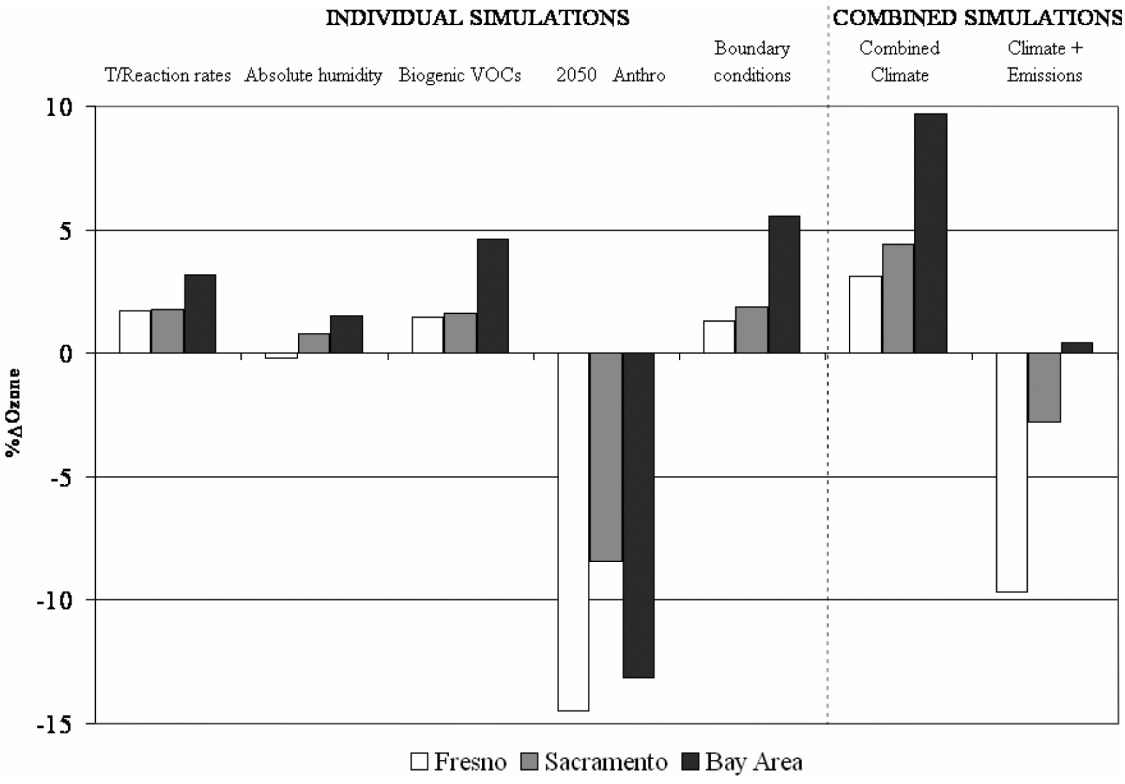

Figure 13. Weekday 1500 LT percent change in weekday maximum ozone concentration, based on spatial averages for three regions: Fresno, Sacramento, and the Bay area. Positive values represent concentrations that are greater in the perturbed case than the base case. The "combined climate" simulation includes the temperature, humidity and biogenic VOC changes. The "climate + emissions" simulation includes temperature, humidity, biogenic VOC, 2050 anthropogenic emissions, and boundary condition changes.

the frequency of stagnation events. In the Sacramento area from the year 2000 to present, the number of exceedance days range from 35 to 60 days per year for the state 1-hour average of 90 ppb, and 25 to 45 days per year for the national 8-hour standard (80 ppb). In the San Francisco Bay area, there are typically less than 20 days per year where the 1-hour state average is exceeded and less than 10 days per year that exceed the national 8-hour average [*California Air Resources Board*, 2005]. The Bay area is not a region typically associated with high ozone in California, however, this work indicates that it may be particularly sensitive to future climate and anthropogenic emissions changes. These three regions tend to have varying amounts of primary emissions, with the greatest NOx emissions occurring in the Bay Area, followed by Sacramento and then Fresno. Typically, Fresno NOx concentrations are approximately half of those in the Bay area.

[49] Figure 13 compares the percent change in ozone for the three selected regions and each of the seven simulations: temperature, absolute humidity, biogenic VOC emissions, anthropogenic emissions, chemical boundary conditions, and the two combined simulations (the combined climate and the total combined simulations). In each case, we calculate the percent change in ozone as compared to the base case simulation, averaged spatially over all of the grid points within the selected region and temporally by averaging the three weekday maximum concentrations (occurring at 1500 LT). Overall, we see that in all regions the climate change perturbation runs (temperature, absolute humidity, and increases in biogenic VOC emissions resulting from temperature changes) tend to be similar (1–5% change), where the specific humidity perturbation has the smallest impact, followed by a greater impact of temperature, and an even larger change in ozone for the biogenic VOC case. In each simulation, there is a 1–2% larger effect in the Bay area for every component of the climate perturbation. Our projected anthropogenic emission reductions are responsible for a larger ozone change than any other individual component of the future scenario and typically result in an 8–14% reduction in ozone. Figure 13 and the following discussion are ordered from relatively low to high NOx regions, where Fresno has the lowest average daytime NOx concentrations and the Bay area has the highest.

[50] In the San Joaquin Valley, ozone in the city of Fresno is slightly affected by climate change. Absolute humidity leads to a slight decrease in ozone (−0.2%), while temperature and biogenic VOC effects each lead to a 1.5–2% increase in ozone. As this region is situated further inland, the western boundary condition changes cause only a 1% increase in ozone. In contrast, emissions reductions have a large effect, reducing the daily ozone maximum by about

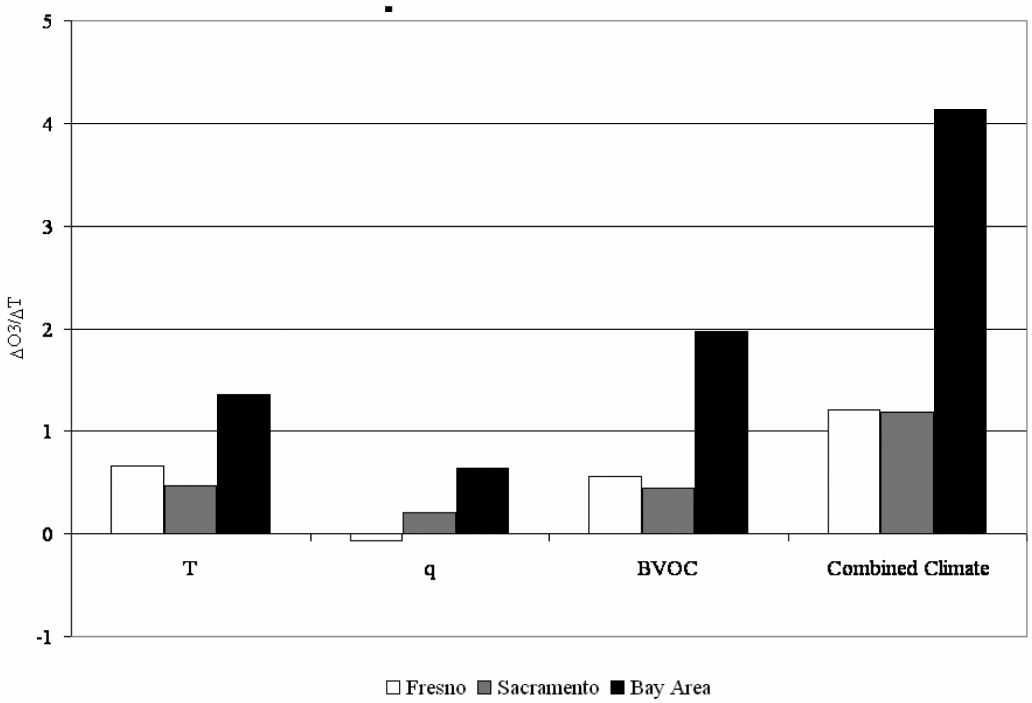

Figure 14. Normalized change in ozone (ppb) per degree temperature at 1500 LT. Each case represents the same temperature change for each region: Fresno $\Delta T = 2.39°C$, Sacramento $\Delta T = 2.44°C$, and the Bay area $\Delta T = 2.08°C$.

14%. The combined effect of these climate perturbations (T, q and biogenic VOC simulations) results in a 3% increase in ozone, while the total combined simulation resulted in a 10% decrease in ozone. This indicates that the impacts of climate change in this region are not as significant as projected emissions reductions.

[51] In Sacramento, temperature effects on reaction rates alone cause a 2% increase in ozone, with lesser changes due to relative humidity (~1%) and biogenic VOC emissions (~1.5%). Changes at the western boundary have a similar effect on ozone, causing a 2% increase. In this case, Sacramento is slightly influenced by the western boundary as air from San Francisco Bay is transported to Sacramento. However, the greatest impact in Sacramento is the 8% reduction in the daily ozone maximum due to anthropogenic emissions reductions. This reduction in ozone due to the anthropogenic emissions reductions carries through to the combined run, with an enhancement of the effect in the combined run. In the combined climate run, ozone increases almost 5% while this change is mitigated by anthropogenic emissions reductions in the climate and emissions simulation, yielding an overall ozone decrease of 3%.

[52] Points to the south and east of San Francisco Bay are more sensitive to expected climate changes than the two regions discussed above. Here, ozone responds more strongly to increases of temperature and biogenic VOCs (3–5% increase each) because the region is NOx-saturated. Additionally, the Bay area is particularly sensitive to inflow boundary conditions because of its proximity to the ocean. Projected anthropogenic emissions reductions are also more effective in the Bay area than other regions, reducing maximum daily ozone concentrations by about 13%. The combined climate effects run results in nearly a 10% increase in ozone, indicating that climate change effects alone will have a strong impact on daily maximum ozone concentrations. Aggressive local emissions reductions in the climate and emissions simulation counteract this change, but in effect lead to no net change in ozone. This indicates that significant anthropogenic emission reductions in the region will be essential to mitigate the consequence of climate change on air quality and illustrates the limitations of local control strategies.

[53] Another approach to evaluate the response of ozone to changing climate is to normalize ozone changes to changes in temperature (Figure 14). Three of our individual perturbation simulations and one combined simulation are driven solely by a change in temperature: (1) the temperature case, where reaction rates change as a function of temperature; (2) absolute humidity, where an increase in atmospheric moisture occurs as a function of temperature increase; and (3) biogenic VOC emissions, where temperature causes an increase in these natural emissions and (4) the combined climate simulation including these three temperature impacts. For the same three geographic regions, we compare the change in ozone per change in temperature (similarly, averaged spatially over each region and temporally over the three weekday maximum). The average 1500 LT temperature increase is 2.4°C in Fresno and Sacramento and 2.1°C in the Bay area. The sensitivity of ozone to temperature in the Bay area is relatively large compared to the other regions. For each of the three individual scenarios, ozone in the Bay area increases about 0.5–2 ppb per degree increase in temperature. In contrast, Sacramento and Fresno see more modest increases on the

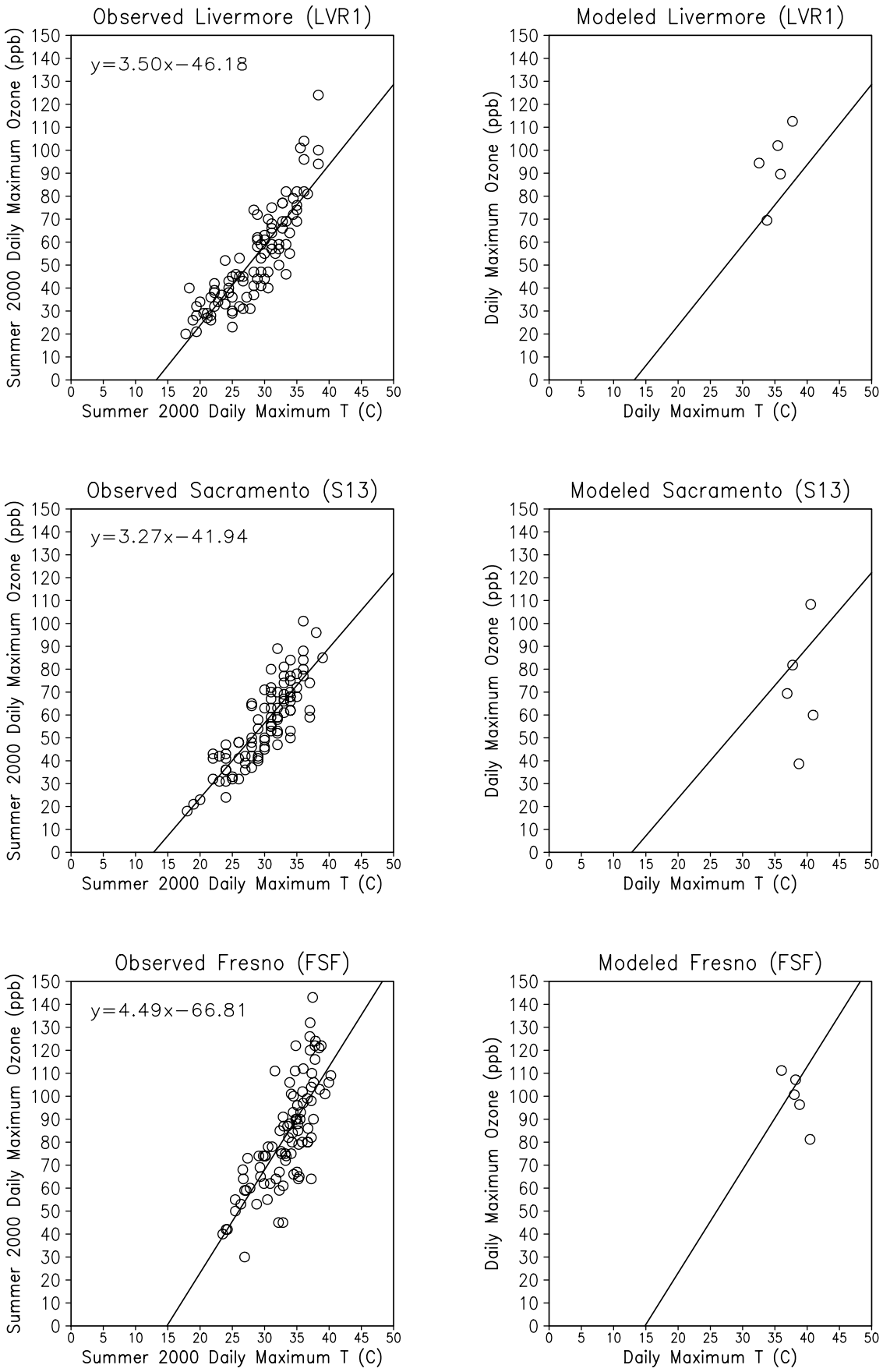
Observed Livermore (LVR1)
y=3.50x−46.18
Summer 2000 Daily Maximum Ozone (ppb)
Summer 2000 Daily Maximum T (C)
Modeled Livermore (LVR1)
Daily Maximum Ozone (ppb)
Daily Maximum T (C)
Observed Sacramento (S13)
y=3.27x−41.94
Summer 2000 Daily Maximum Ozone (ppb)
Summer 2000 Daily Maximum T (C)
Modeled Sacramento (S13)
Daily Maximum Ozone (ppb)
Daily Maximum T (C)
Observed Fresno (FSF)
y=4.49x−66.81
Summer 2000 Daily Maximum Ozone (ppb)
Summer 2000 Daily Maximum T (C)
Modeled Fresno (FSF)
Daily Maximum Ozone (ppb)
Daily Maximum T (C)

Figure 15

order of 0.2–0.7 ppb, with a slight decrease in Fresno for the specific humidity case. In the case of the increase in temperature and absolute humidity runs, impacts of temperature in the Bay area are double those on Sacramento and Fresno. In the biogenic VOC case, the impacts in the Bay area are triple those in the other regions. The sensitivities of the three regions order with NOx emissions and VOC/NOx ratios (the average weekday 1500 LT VOC/NOx ratio for the Bay area is 1.8, with a value of 2 in Sacramento and 5 in Fresno). In the combined climate simulation, ozone increases about 1 ppb per degree temperature in Sacramento and Fresno, and 4 ppb per degree temperature in the Bay Area, indicating a much stronger combined response to temperature.

[54] In order to examine if modeled sensitivities to temperature are similar to those observed in California, we examine the observed ozone record during the summer of 2000. Ground-based observations from a site within each region (Fresno, Sacramento, and Livermore in the Bay Area) illustrate the seasonal relationship between the daily maximum temperature and daily maximum ozone concentration (Figure 15, left), where slopes are determined using a least squares regression. Fresno exhibits the greatest sensitivity of ozone to temperature, followed by the Livermore site in the Bay Area and the Sacramento site. Modeled relationships for the 5-day base case simulation are shown in Figure 15 (right) for grid cells that match the observation locations with the observed least squares regression. While we do not have enough data from the 5-day simulation for a complete comparison, the observed relationships indicate that the model may be underestimating the temperature sensitivity in some regions. This may be true particularly in the San Joaquin Valley, although a seasonal simulation could provide more insight into the relationships between temperature and ozone in the model.

[55] There is a large degree of uncertainty implicit in future predictions of emissions and climate. Future climate scenarios can create an array of temperature perturbations with a wide range of impacts and synergistic effects on modeled air quality. Future emissions scenarios are dependent upon global and regional emission reductions policies, and different scenarios could change VOC/NOx ratios with varying impacts on ozone. The boundary condition simulation indicates that the western coast of the United States will also be susceptible to impacts from intercontinental transport, and there is a large amount of uncertainty in the upwind concentrations of precursor emissions and the evolution of plumes across the Pacific due to the complex interplay of growing population and changing policies in Asia. Additionally, there is still uncertainty with respect to the prediction of present-day ozone and the effectiveness of air quality models for this purpose as indicated by the discrepancies between measured and modeled ozone sensitivities. In this study, we use the model to represent a single ozone episode in central California, and the outcomes may vary slightly depending on the type of ozone event present. However, despite the model limitations, the scenarios selected in this study examine several possible outcomes of future emission and climate scenarios and provide insight into the regional gas phase chemistry and chemical mechanisms for a range of scenarios. These results represent likely mechanisms for the interactions of atmospheric chemistry and climate in California's future. Additionally, these results can be applied to other geographic regions with similar baseline chemistry. For example, ozone changes and temperature sensitivities (Figures 13 and 14) can be applied to other urban regions with similar VOC/NOx emission ratios and ozone chemistry and may be useful in determining effective emission reductions policies.

6. Conclusions

[56] In this study, we evaluated the impact of individual physical and chemical perturbations on ozone formation in central California. We find that changes in climate variables, including temperature and atmospheric moisture, cause increases to peak ozone concentrations on the order of a few ppb. Climatically influenced biogenic emissions cause ozone increases of a similar magnitude. Other chemical changes, such as the increase of concentrations at the western boundary, can cause greater changes in ozone depending on proximity to the boundary and other geographic features, e.g., the strong impact on the San Francisco Bay area. We predict reductions in anthropogenic emissions in 2050 on the basis of assumptions regarding future technologies and growth, setting an aggressive target for air quality control regulatory policies. These reductions lead to ozone decreases of 10–20 ppb in urban areas and represent the greatest single potential impact on ozone concentrations. NOx reductions of 10–20% are not large enough to be effective at ozone reduction, but VOC and CO emission reductions in NOx-saturated regions are effective at reducing ozone. In fact, because of the nonlinearities, these small NOx reductions likely offset some of the benefit of VOC reductions.

[57] When evaluating the combined effects of these perturbations, we find that the overall impact varies greatly by region with strong correlation to NOx concentrations and proximity to the coastline. This modeling study indicates that regions such as the San Francisco Bay area are more sensitive than others to climate change, and climate change impacts are likely to negate many of the benefits of projected emissions reductions. However, in the Central Valley, anthropogenic emissions reductions are predicted to be effective, despite a slight decrease in their efficacy due to climatic changes. These results indicate that the benefits of aggressive emissions reductions will be overstated if climatic changes are not accounted for in projections.

Figure 15. Observed and modeled relationships between ozone and temperature. (left) Observed relationship between ozone and temperature at three sites in the delineated regions (Livermore in the Bay Area, Sacramento, and Fresno), using the daily maximum temperature and ozone measurements from the entire 2000 ozone season (1 July to 1 October). (right) Modeled relationship between the daily maximum surface ozone and temperature for the 5-day base case simulation for the grid cell of each measurement location. Circles represent daily maxima for observed or modeled data, and the line displays the least squares regression for the observed data.

[58] Finally, this study indicates that geographic regions of concern with respect to air quality may shift in the future. In central California, current efforts to improve air quality are mainly focused on the Central Valley. In the future, the San Francisco Bay area may be particularly sensitive to climate change despite strong reductions in anthropogenic emissions. In this region, the severity and frequency of ozone episodes may increase, causing more annual ozone exceedances. These results indicate that the challenge of predicting future air quality will include understanding the balance between anthropogenic emissions reductions and the impact of climate change.

[59] **Acknowledgments.** Although the research described in this article has been funded wholly or in part by the U.S. Environmental Protection Agency through grant RD-83096401-0 to the University of California, Berkeley, it has not been subjected to the Agency's required peer and policy review and therefore does not necessarily reflect the view of the Agency and no official endorsement should be inferred. We thank two anonymous reviewers for their helpful suggestions and comments.

References

Altschuler, S. L., T. D. Arcado, and D. R. Lawson (1995), Weekday versus weekend ambient ozone concentrations: Discussion and hypotheses with focus on Northern California, *J. Air Waste Manage. Assoc.*, *45*, 967–972.

Aw, J., and M. J. Kleeman (2003), Evaluating the first-order effect of intraannual temperature variability on urban air pollution, *J. Geophys. Res.*, *108*(D12), 4365, doi:10.1029/2002JD002688.

Brasseur, G. P., J. T. Kiehl, J. F. Muller, T. Schneider, C. Granier, X. X. Tie, and D. Hauglustaine (1998), Past and future changes in global tropospheric ozone: Impact on radiative forcing, *Geophys. Res. Lett.*, *25*(20), 3807–3810.

Byun, D. W., and J. K. S. Ching (1999), Science algorithms of the EPA Models-3 Community Multiscale Air Quality (CMAQ) modeling system, *EPA/600/R-99/030*, U.S. Environ. Prot. Agency, Washington, D. C.

California Air Resources Board (2005), Statewide trends and forecasts—Criteria pollutants, in *ARB Almanac 2005*, chap. 3, pp. 88–110, Sacramento, Calif. (Available at http://arb.ca.gov/aqd/almanac/almanac05/pdf/chap305.pdf)

California Department of Finance (2004), Populations projections by race/ethnicity for California and its counties, 2000–2050, Sacramento, Calif., May. (Available at http://www.dof.ca.gov/HTML/DEMOGRAP/ReportsPapers/Projections/P1/P1.asp)

Cardelino, C. A., and W. L. Chameides (1990), Natural hydrocarbons, urbanization and urban ozone, *J. Geophys. Res.*, *95*, 13,971–13,979.

Carter, W. P. L. (2000), Implementation of the SAPRC-99 Chemical Mechanism into the Models-3 Framework, report, U.S. Environ. Prot. Agency, Washington, D. C.

Cleveland, W. S., T. E. Graedel, B. Kleiner, and J. L. Warner (1974), Sunday and workday variations in photochemical air pollutants in New Jersey and New York, *Science*, *186*, 1037–1038.

Coquard, J., P. B. Duffy, K. E. Taylor, and J. P. Iorio (2004), Present and future surface climate in the western USA as simulated by 15 global climate models, *Clim. Dyn.*, *23*(4), 455–472.

Fujita, E., D. Campbell, R. Keislar, and J. Bowan (2001), *Central California Ozone Study (CCOS)*, vol. III, *Summary of Field Operations*, final report, Calif. Air Resour. Board, Sacramento, Calif.

Goldan, P. D., W. C. Kuster, F. Fehsenfeld, and S. A. Montzka (1993), The observation of a C5 alcohol emission in a North American pine forest, *Geophys. Res. Lett.*, *20*, 1039–1042.

Goldstein, A. H., et al. (2004), Impact of Asian emissions on observations at Trinidad Head, California during ITCT 2K2, *J. Geophys. Res.*, *109*, D23S17, doi:10.1029/2003JD004406.

Guenther, A., et al. (1995), A global model of natural volatile organic compound emissions, *J. Geophys. Res.*, *100*(D5), 8873–8892.

Harley, R. A., L. C. Marr, J. K. Lehner, and S. N. Giddings (2005), Changes in motor vehicle emissions on diurnal to decadal time scales and effects on atmospheric composition, *Environ. Sci. Technol.*, *39*, 5356–5362.

Hayhoe, K., et al. (2004), Emission pathways, climate change, and impacts on California, *Proc. Natl. Acad. Sci. U. S. A.*, *101*(34), 12,422–12,427.

Hogrefe, C., B. Lynn, K. Civerolo, J.-Y. Ku, J. Rosenthal, C. Rosenzweig, R. Goldberg, S. Gaffin, K. Knowlton, and P. L. Kinney (2004), Simulating changes in regional air pollution over the eastern United States due to changes in global and regional climate and emissions, *J. Geophys. Res.*, *109*, D22301, doi:10.1029/2004JD004690.

Holloway, T. A., A. M. Fiore, and M. G. Hastings (2003), Intercontinental transport of air pollution: Will the emerging science lead to a new hemispheric treaty?, *Environ. Sci. Technol.*, *37*, 4535–4542.

Hudman, R. C., et al. (2004), Ozone production in transpacific Asian pollution plumes and implications for ozone air quality in California, *J. Geophys. Res.*, *109*, D23S10, doi:10.1029/2004JD004974.

Intergovernmental Panel on Climate Change (2001), *Climate Change 2001: The Scientific Basis*, edited by J. T. Houghton et al., 944 pp., Cambridge Univ. Press, New York.

Jacob, D. J., et al. (1993), Factors regulating ozone over the United States and its export to the global atmosphere, *J. Geophys. Res.*, *98*(D8), 14,817–14,826.

Jacob, D. J., J. A. Logan, and P. P. Murti (1999), Effect of rising Asian emissions on surface ozone in the United States, *Geophys. Res. Lett.*, *26*(14), 2175–2178.

Jacobson, M., and R. P. Turco (1994), SMVGEAR: A sparse-matrix, vectorized gear code for atmospheric models, *Atmos. Environ.*, *28*, 273–284.

Johnson, C. E., W. J. Collins, D. S. Stevenson, and R. G. Derwent (1999), Relative roles of climate and emissions changes on future tropospheric oxidant concentrations, *J. Geophys. Res.*, *104*(D15), 18,631–18,645.

Kleinman, L. I. (1986), Photochemical formation of peroxides in the boundary layer, *J. Geophys. Res.*, *91*, 10,889–10,904.

Kleinman, L. I. (1994), Low and high-NOx tropospheric photochemistry, *J. Geophys. Res.*, *99*, 16,831–16,838.

Lamanna, M. S., and A. H. Goldstein (1999), In situ measurements of a C2–C10 volatile organic compounds above a Sierra Nevada ponderosa pine plantation, *J. Geophys. Res.*, *104*(D7), 21,247–21,262.

Leung, L. R., and W. I. Gustafson Jr. (2005), Potential regional climate change and implications to U.S. air quality, *Geophys. Res. Lett.*, *32*, L16711, doi:10.1029/2005GL022911.

Marr, L. C., and R. A. Harley (2002), Spectral analysis of weekday-weekend differences in ambient ozone, nitrogen oxide, and non-methane hydrocarbon time series in California, *Atmos. Environ.*, *36*, 2327–2335.

Marr, L. C., D. R. Black, and R. A. Harley (2002), Formation of photochemical air pollution in Central California. I. Development of a revised motor vehicle emission inventory, *J. Geophys. Res.*, *107*(D6), 4047, doi:10.1029/2001JD000689.

Mickley, L. J., D. J. Jacob, B. D. Field, and D. Rind (2004), Effects of future climate change on regional air pollution episodes in the United States, *Geophys. Res. Lett.*, *31*, L24103, doi:10.1029/2004GL021216.

National Research Council (1991), *Rethinking the Ozone Problem in Urban and Regional Air Pollution*, Natl. Acad. Press, Washington, D. C.

Parrish, D. D., et al. (2004), Changes in the photochemical environment of the temperate North Pacific troposphere in response to increased Asian emissions, *J. Geophys. Res.*, *109*, D23S18, doi:10.1029/2004JD004978.

Prather, M., et al. (2003), Fresh air in the 21st century?, *Geophys. Res. Lett.*, *30*(2), 1100, doi:10.1029/2002GL016285.

Sanderson, M. G., C. D. Jones, W. J. Collins, C. E. Johnson, and R. G. Derwent (2003), Effect of climate change on isoprene emissions and surface ozone levels, *Geophys. Res. Lett.*, *30*(18), 1936, doi:10.1029/2003GL017642.

Scott, K. I., and M. T. Benjamin (2003), Development of a biogenic volatile organic compound emission inventory for the SCOS97–NARSTO domain, *Atmos. Environ.*, *37*(2), S39–S49.

Sillman, S. (1995), The use of NOy, H_2O_2, and HNO_3 as indicators for ozone-NOx-hydrocarbon sensitivity in urban locations, *J. Geophys. Res.*, *100*(D7), 14,175–14,188.

Sillman, S., and F. J. Samson (1995), Impact of temperature on oxidant photochemistry in urban, polluted rural and remote environments, *J. Geophys. Res.*, *100*(D6), 11,497–11,508.

Sillman, S., J. A. Logan, and S. C. Wofsy (1990), The sensitivity of ozone to nitrogen oxides and hydrocarbons in regional ozone episodes, *J. Geophys Res.*, *95*, 1837–1851.

Snyder, M. A., J. L. Bell, L. C. Sloan, P. B. Duffy, and B. Govindasamy (2002), Climate responses to a doubling of atmospheric carbon dioxide for a climatically vulnerable region, *Geophys. Res. Lett.*, *29*(11), 1514, doi:10.1029/2001GL014431.

Talbot, R., et al. (2003), Reactive nitrogen in Asian continental outflow over the western Pacific: Results from the NASA Transport and Chemical Evolution over the Pacific (TRACE-P) airborne mission, *J. Geophys. Res.*, *108*(D20), 8803, doi:10.1029/2002JD003129.

Thornton, J. A., et al. (2002), Ozone production rates as a function of NO_x abundances and HO_x production rates in the Nashville urban plume, *J. Geophys. Res.*, *107*(D12), 4146, doi:10.1029/2001JD000932.

U.S. Environmental Protection Agency (2004), 8-hour ground-level ozone designations, Region 9, Washington, D. C. (Available at http://www.epa.gov/ozonedesignations/regions/region9desig.htm)

U.S. Environmental Protection Agency (2005), Air emissions trends—Continued progress through 2004, Washington, D. C. (Available at http://www.epa.gov/airtrends/2005/econ-emissions.html)

Wallace, J. M., and P. V. Hobbs (2006), *Atmospheric Science: An Introductory Survey*, 2nd ed., 504 pp., Elsevier, New York.

Wotawa, G., and M. Trainer (2000), The influence of Canadian forest fires on pollutant concentrations in the United States, *Science*, *288*(5464), 324–328.

R. C. Cohen, Department of Chemistry, University of California, Berkeley, CA 94720-1460, USA.

A. H. Goldstein and A. L. Steiner, Department of Environmental Science, Policy and Management, Division of Ecosystem Sciences, University of California, Berkeley, CA 94720-3110, USA. (asteiner@nature.berkeley.edu)

R. A. Harley, Department of Civil and Environmental Engineering, University of California, Berkeley, CA 94720-1710, USA.

S. Tonse, Environmental Energy Technologies Division, Lawrence Berkeley National Laboratory, Berkeley, CA 94720, USA.